Electronic Supplementary Material (ESI) for Organic & Biomolecular Chemistry.

Synthesis of new *β*-amino acid with 3-deoxy-L-*ara* furnaoside side chain: influence of side chain on the conformation of *α*/*β*-peptides

Gangavaram V. M. Sharma,*[a] Gonuguntla Anjaiah,[a,c] Marumudi Kanakaraju, [b,c] Bommeda Sudhakar,[a] Deepak Chatterjee,[b] and Ajit C. Kunwar*[b]

a. Organic and Biomolecular Chemistry Division, b. Centre for Nuclear Magnetic Resonance, CSIR-Indian Institute of Chemical Technology, Hyderabad 500 007, India

b. Both the authors have made equal contributions

Email: esmvee@iict.res.in; kunwar@iict.res.in

Contents

Determination of absolute stereochemistry of 1	2-3
NMR Spectra	4-37
Molecular Dynamics Studies	38-42
CD Studies	43-44

Determination of absolute stereochemistry of 1

The absolute stereochemistry at the Cβ-carbon in **1** was determined by Mosher's method.[18] Accordingly, amine **10** was subjected to reaction with (*R*)- and (*S*)-α-methoxyphenyl acetic acids **12a** and **12b** independently, to furnish the Mosher amides **13a** (85%) and **13b** (82%) respectively (Supporting Scheme 1).

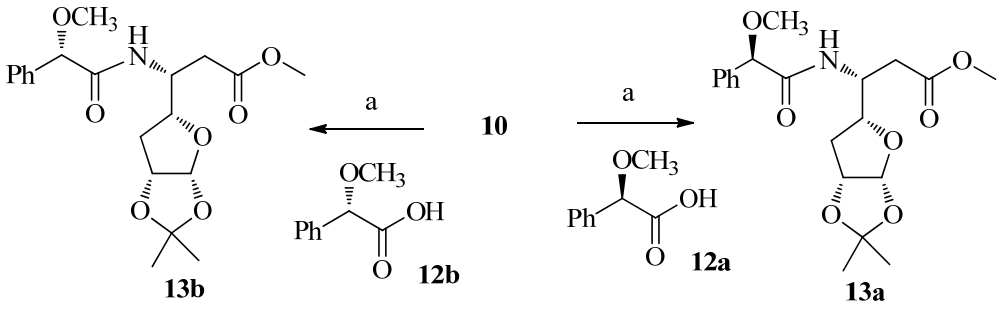

Reagents and conditions : a) HOBt, EDCI, CH_2Cl_2, 0 ºC-rt. 5 h.

Supporting Scheme 1: Synthesis of Mosher amides **13a** and **13b**.

The configuration at Cβ-position in **1** was ascertained by comparison of the chemical shifts and their differences ($\Delta\delta^{RS}$) for various protons in **13a** and **13b** (SupportingTable 1). For **13a**, the resonances for CαH, CαH' and -COOMe shifted upfield (shielded) with ($\Delta\delta^{RS}$) = -0.08, -0.12 and -0.16 ppm respectively, with respect to **13b**.

Supporting Table 1: Chemical shifts (δ ppm) and their differences (Δδ ppm) in amides **13a** and **13b**

	CβH	C4H	C3H	C3H'	C2H	C1H	COOMe	CαH	CαH'
13a	4.46	4.26	2.25	1.99	4.74	5.66	3.51	2.66	2.57
13b	4.38	4.27	2.15	1.86	4.72	5.63	3.67	2.74	2.69
$\Delta\delta^{RS}$	0.08	-0.01	0.10	0.13	0.02	0.03	-0.16	-0.08	-0.12

Likewise, the resonances for CβH, C3H, C3H', C2H and C1H are deshielded and shifted downfield with ($\Delta\delta^{RS}$) = 0.08, 0.10, 0.13, 0.02, and 0.03 ppm respectively, with respect to **13b**. These observations imply that the phenyl group, CαH and -COOMe are in the same plane in (*R*)-MPA, while, the phenyl and C3H, C2H and C1H are in one plane in (*S*)-MPA. This in turn conclusively proves that configuration at the amine stereocentre in the above compound is '*R*'. Supporting Figure 1 shows energy minimized structure of **11**.

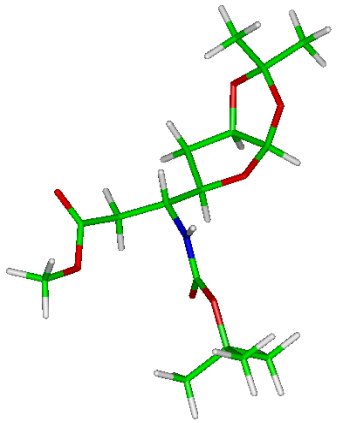

Supporting Figure 1: Energy minimized structure of (*R*)-β-Caa$_{(da)}$ **11**.

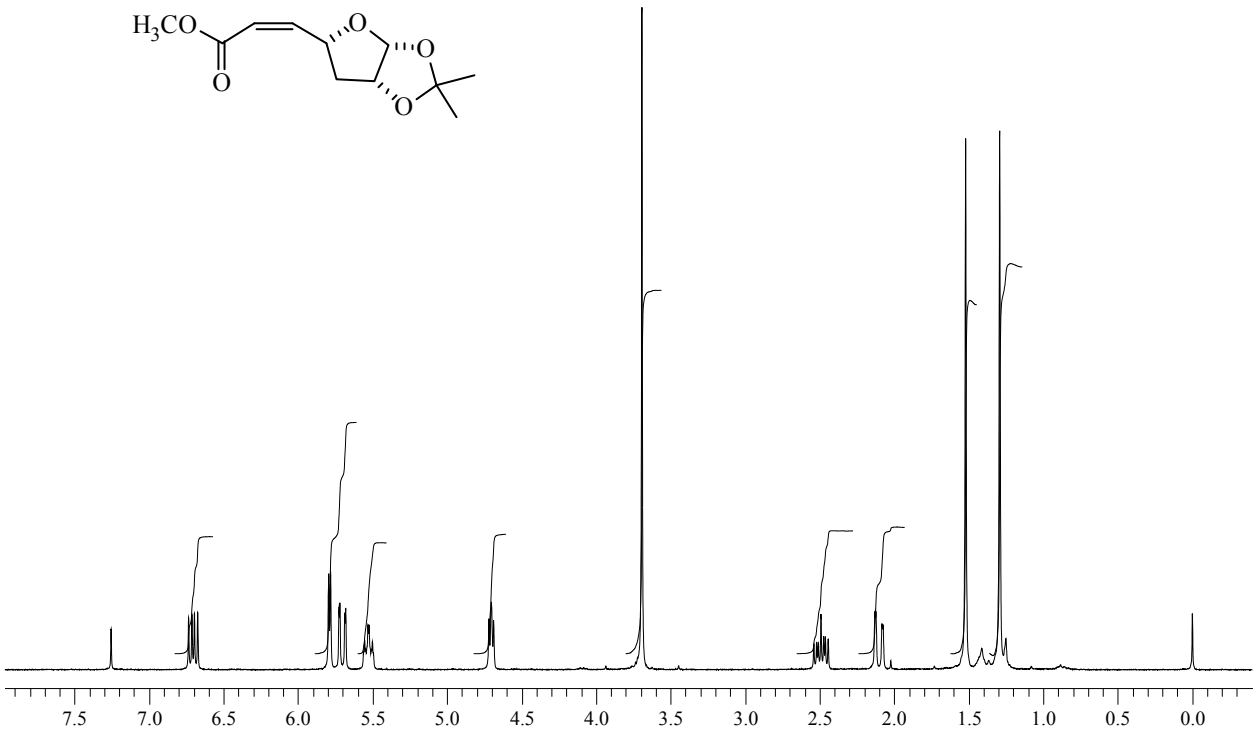

Supporting Figure 2: ^{1}H NMR spetrum of **8a** (300 MHz, $CDCl_3$, 295 K)

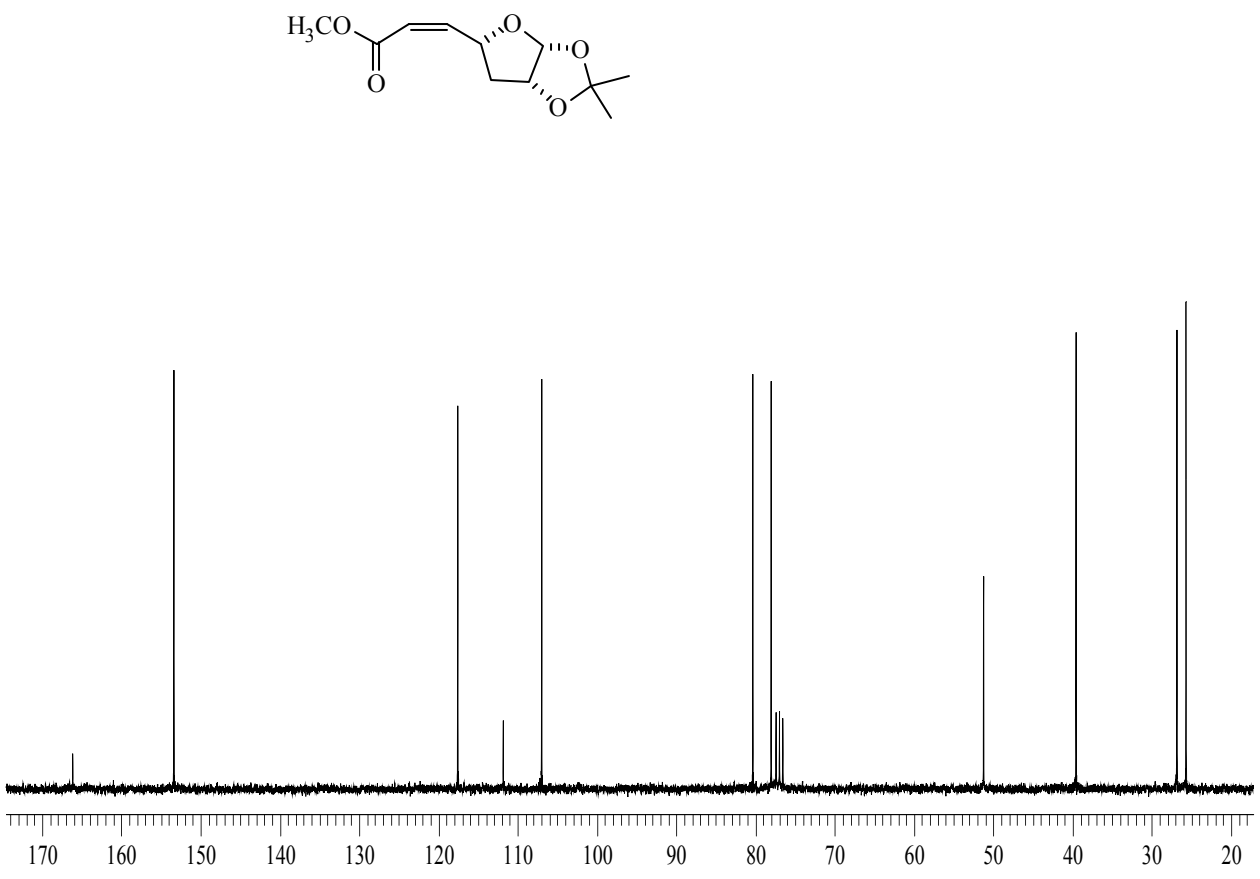

Supporting Figure 3: ^{13}C NMR spetrum of **8a** (75 MHz, $CDCl_3$, 295 K)

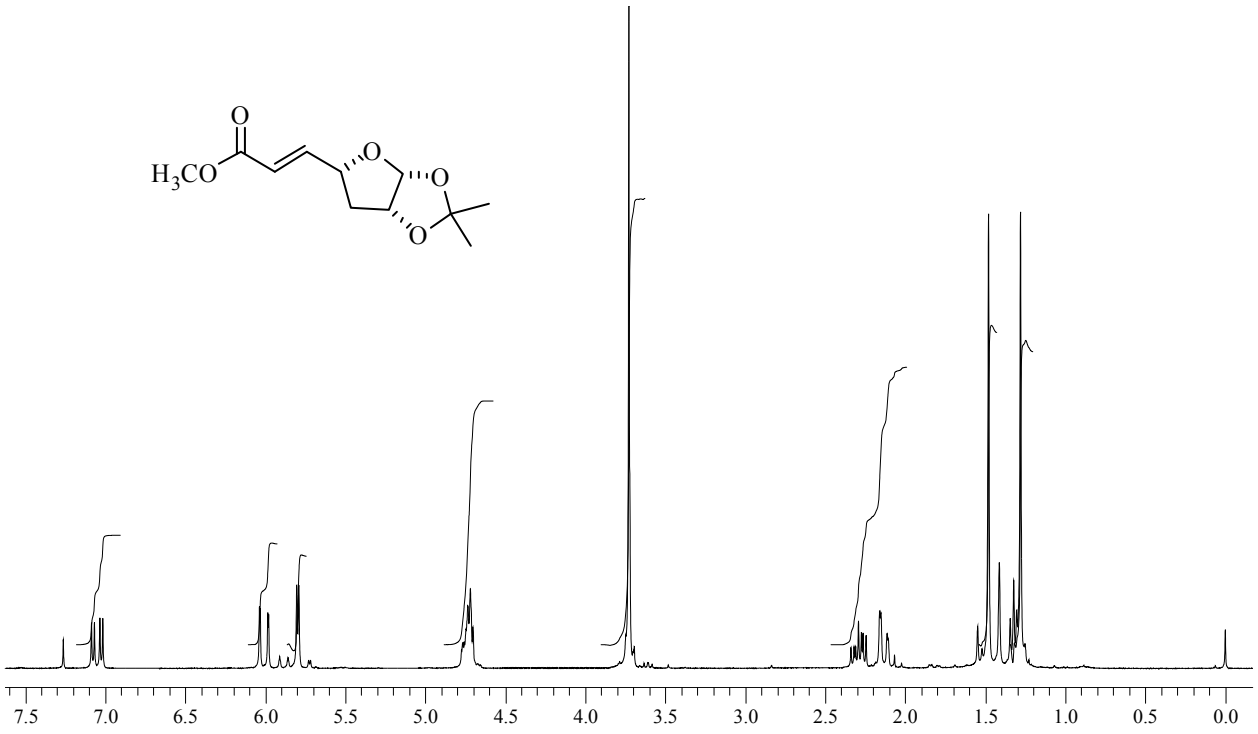

Supporting Figure 4: ^{1}H NMR spetrum of **8b** (300 MHz, $CDCl_3$, 295 K)

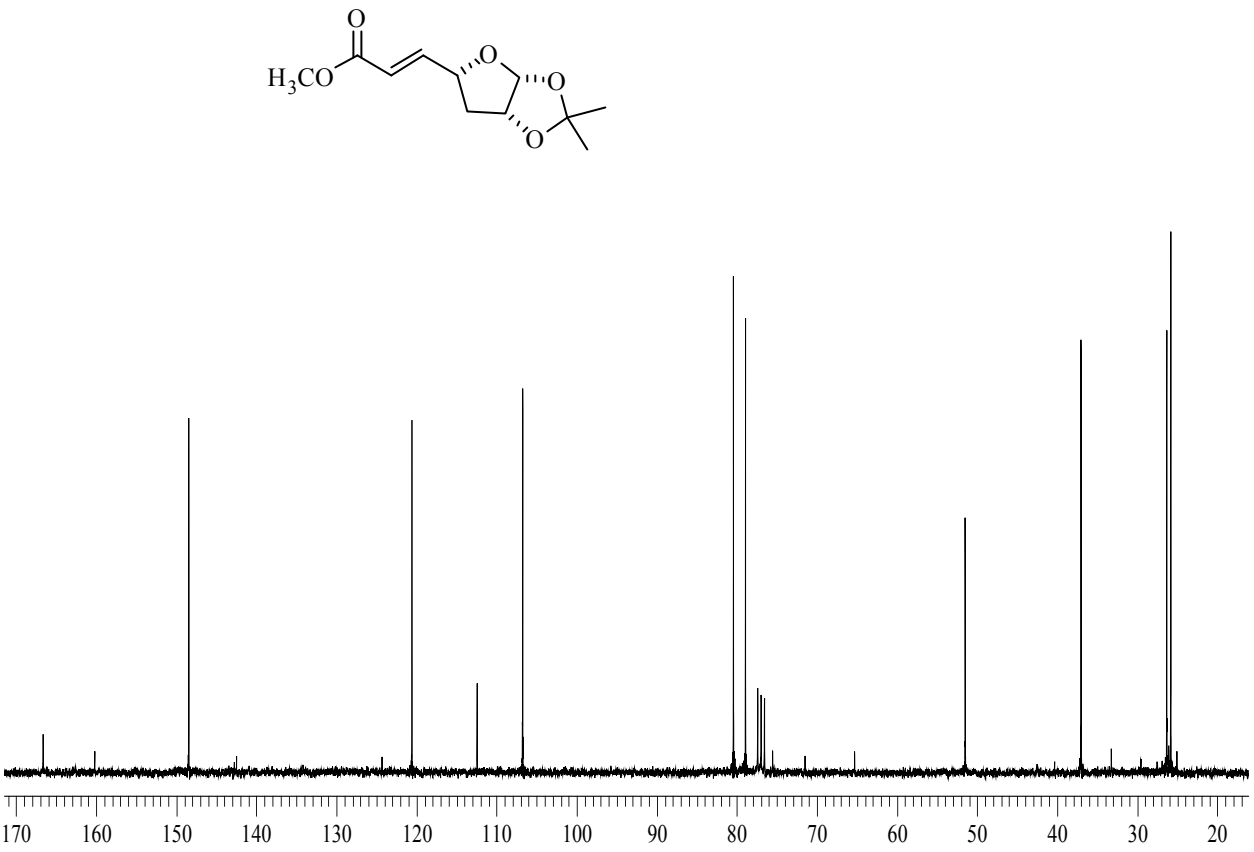

Supporting Figure 5: ^{13}C NMR spetrum of **8b** (75 MHz, $CDCl_3$, 295 K)

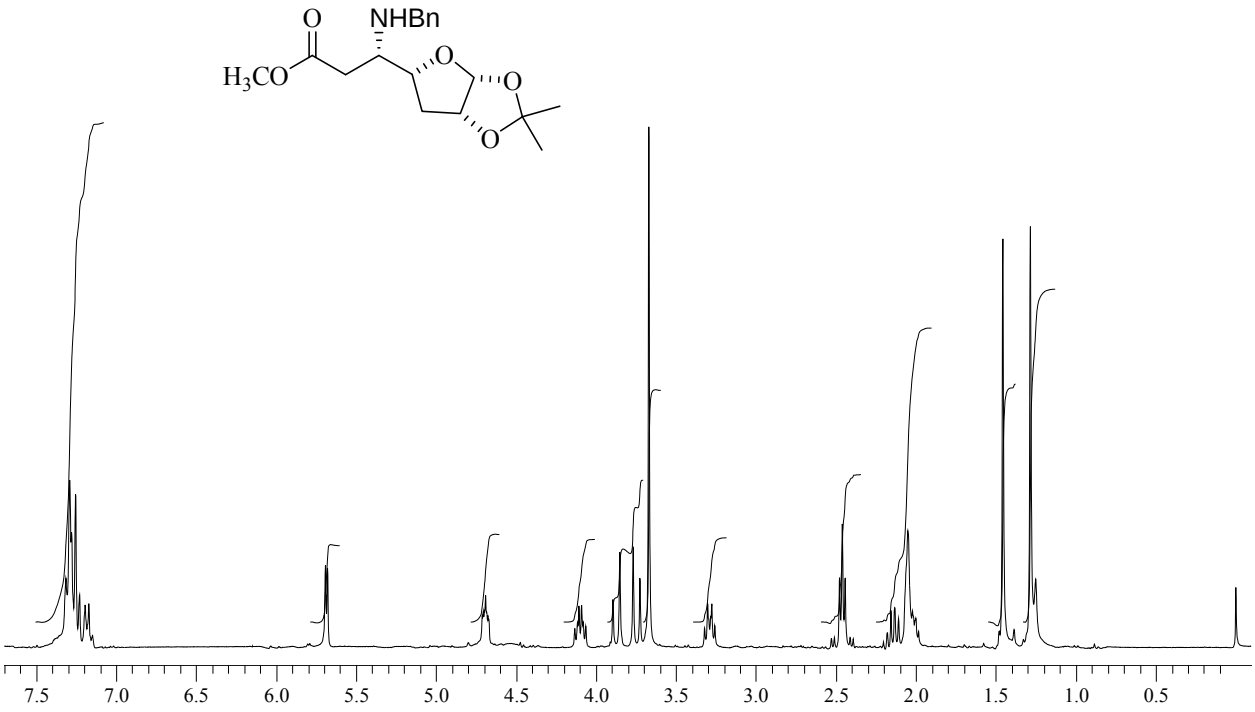

Supporting Figure 6: ^{1}H NMR spetrum of **9a** (300 MHz, $CDCl_3$, 295 K)

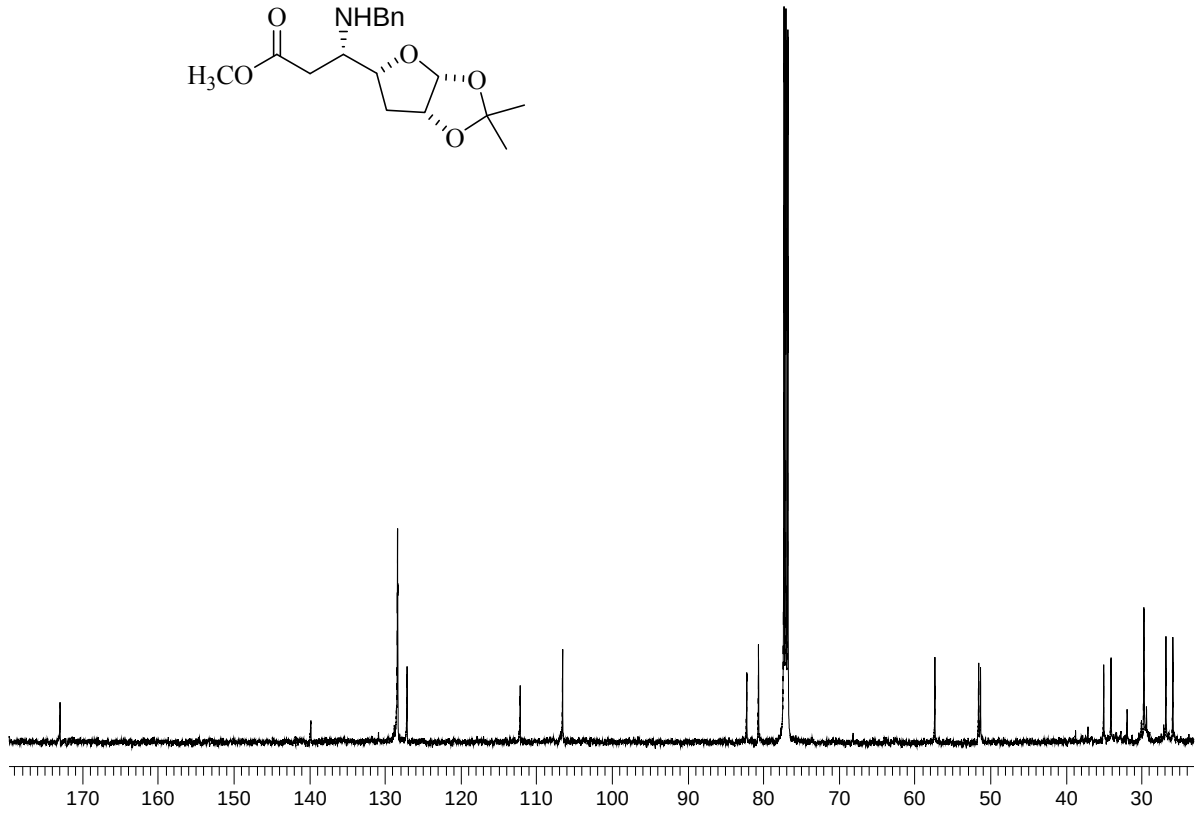

Supporting Figure 7: ^{13}C NMR spetrum of **9a** (75 MHz, $CDCl_3$, 298 K)

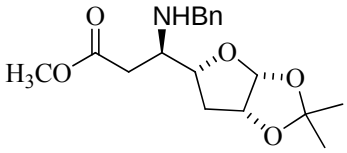

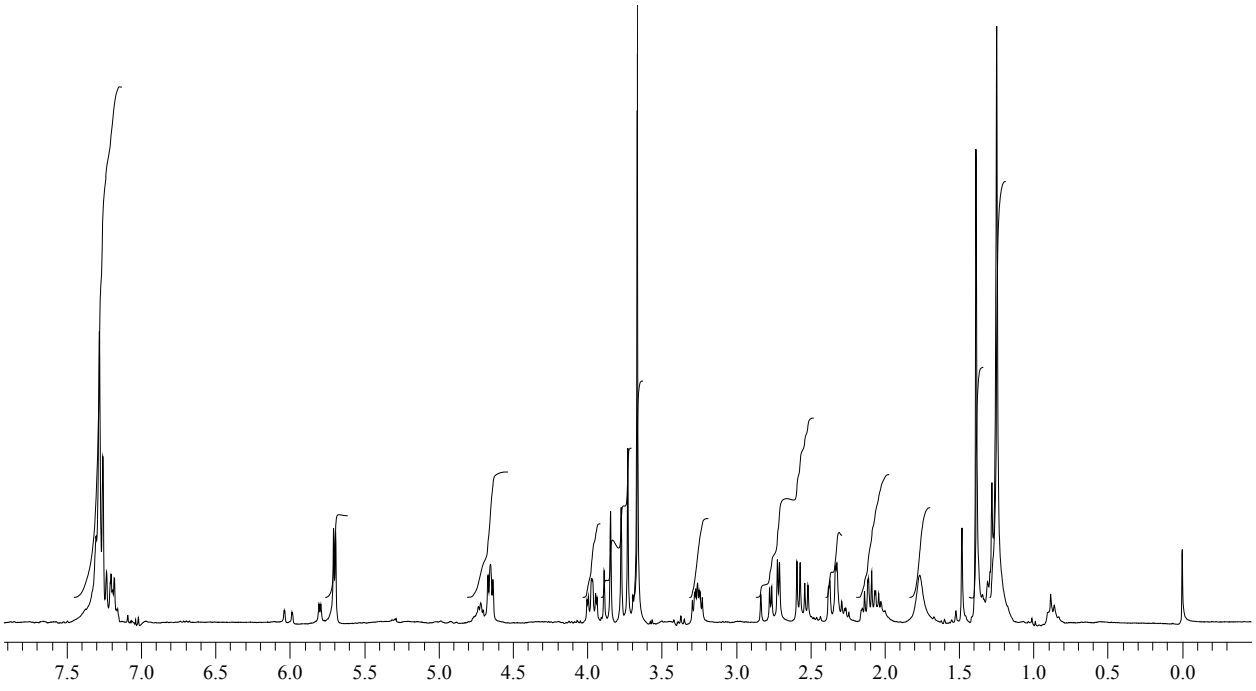

Supporting Figure 8: ^{1}H NMR spetrum of **9b** (300 MHz, $CDCl_3$, 295 K)

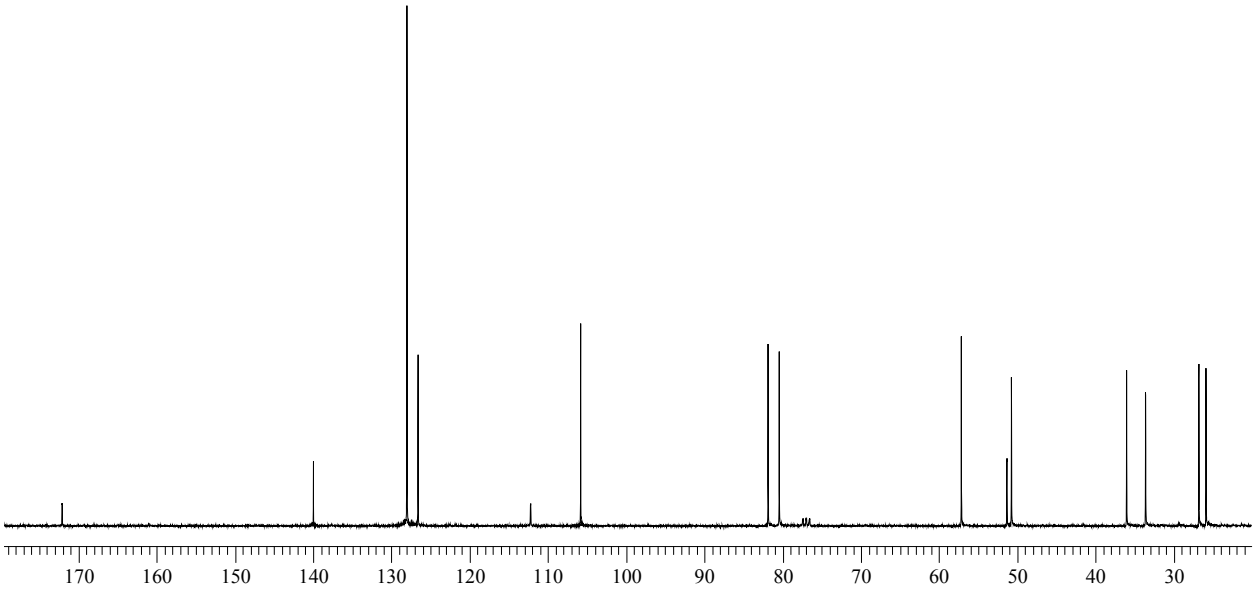

Supporting Figure 9: ^{13}C NMR spetrum of **9b** (75 MHz, $CDCl_3$, 295 K)

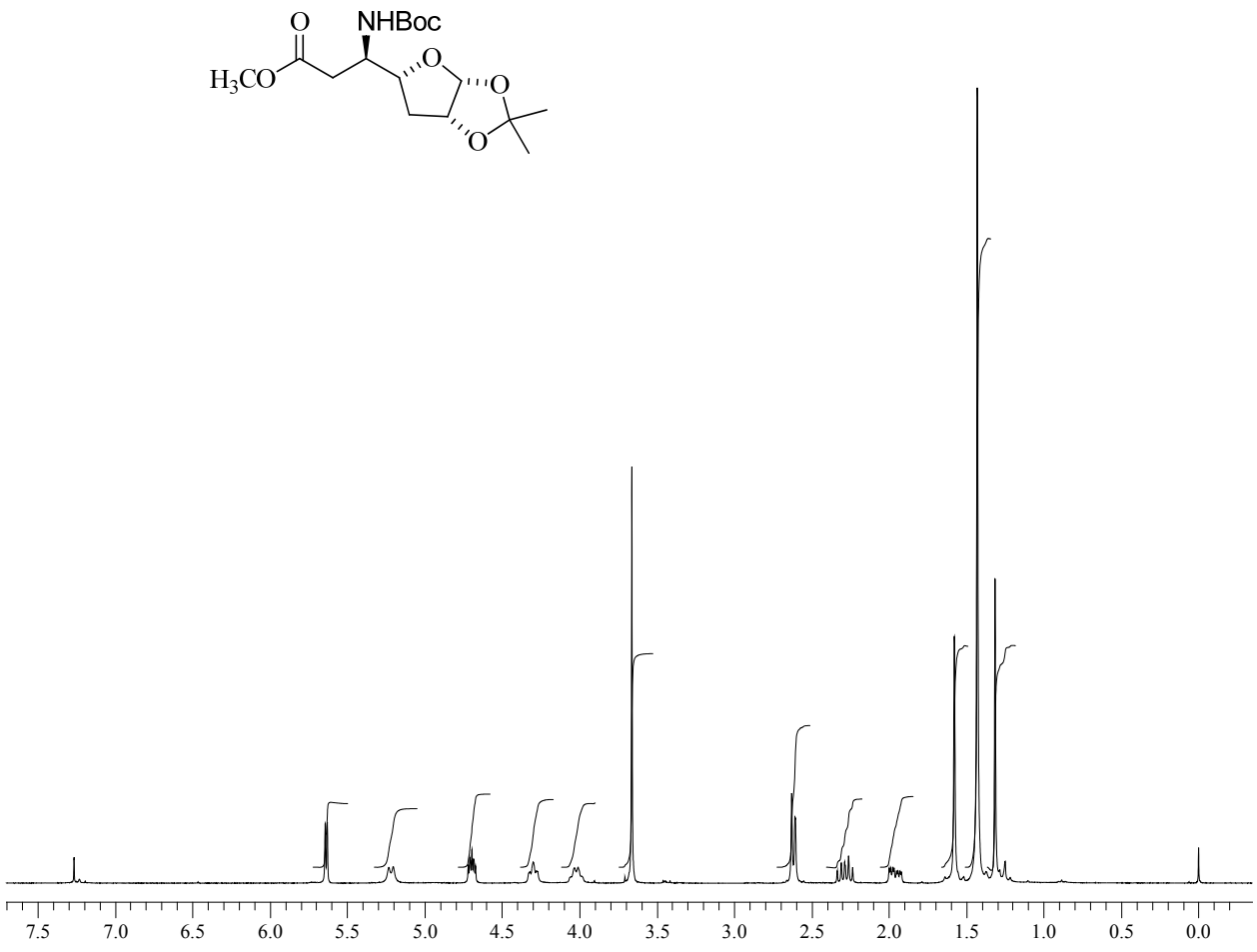

Supporting Figure 10: ^{1}H NMR spetrum of **11** (300 MHz, $CDCl_3$, 295 K)

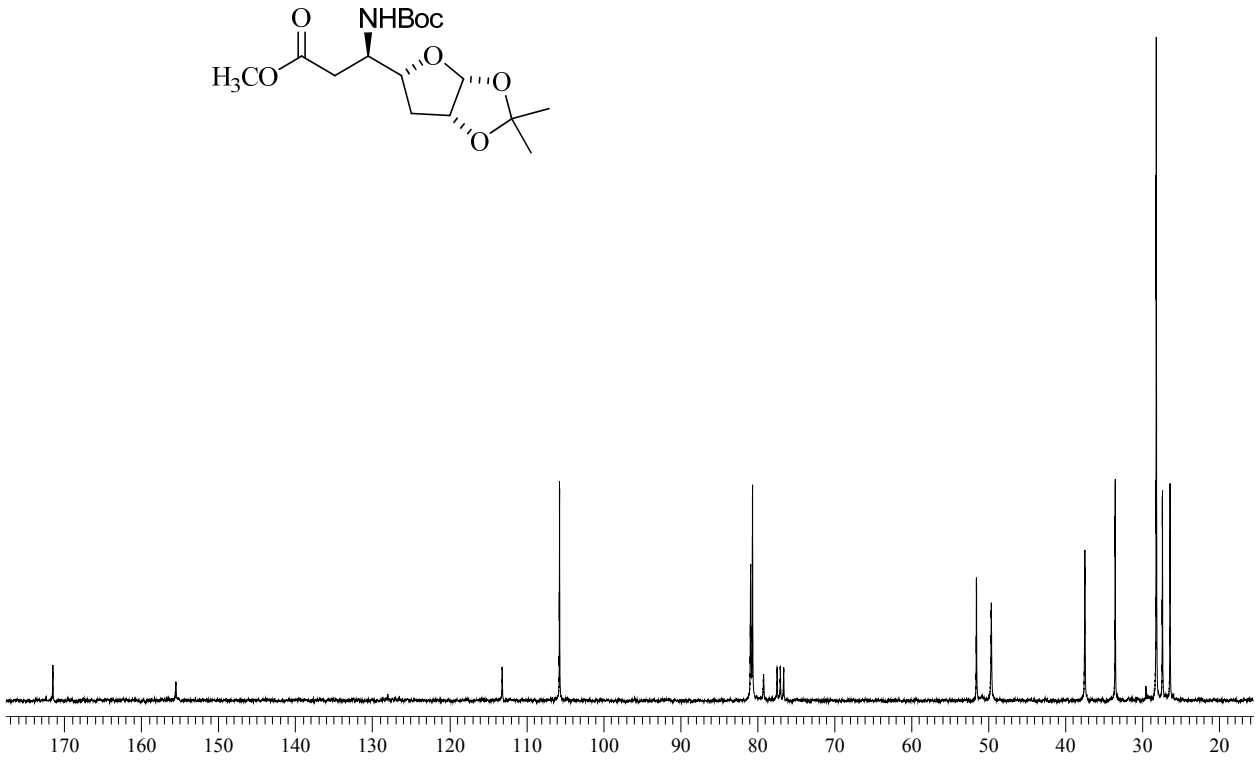

Supporting Figure 11: ^{13}C NMR spetrum of **11** (75 MHz, $CDCl_3$, 295 K)

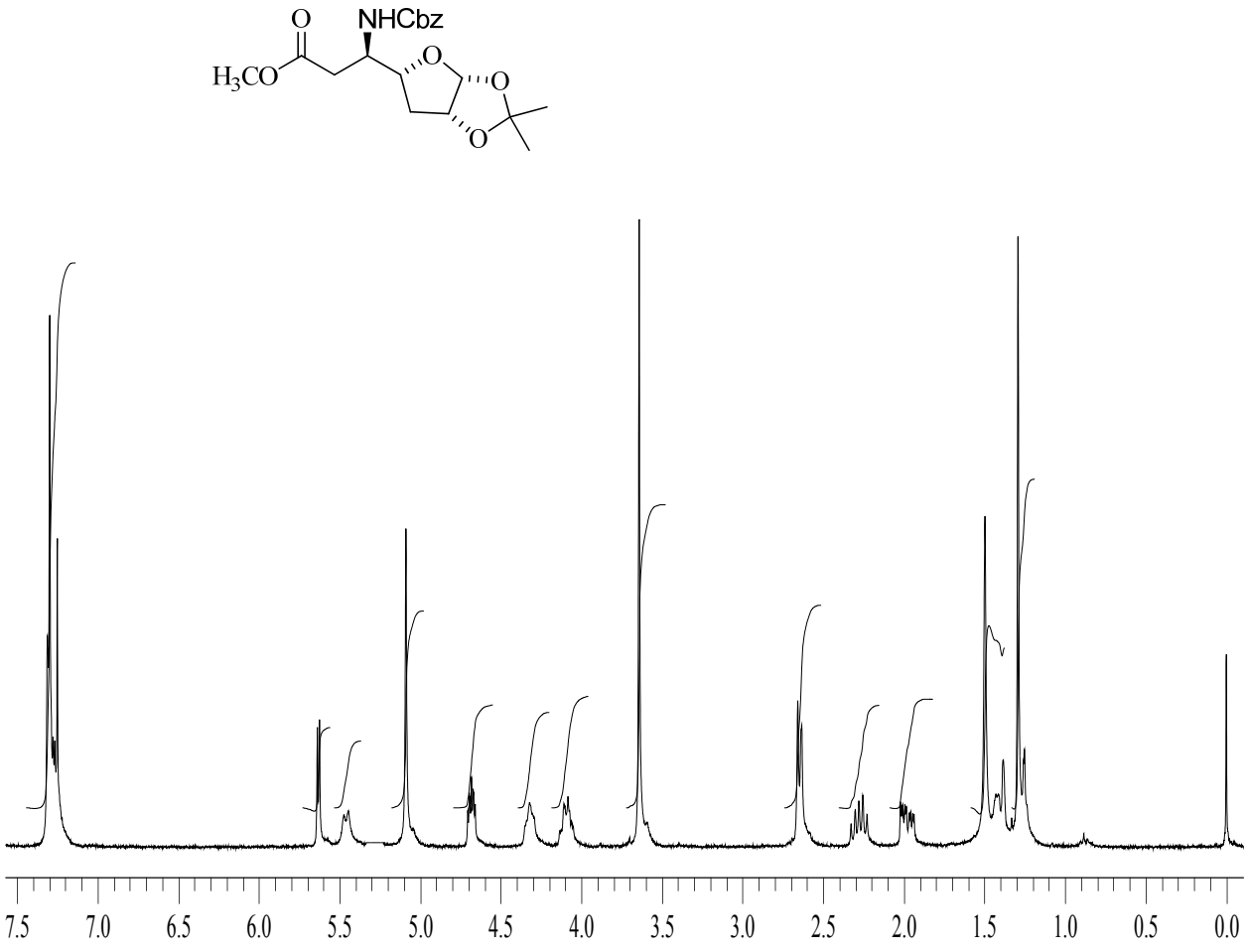

Supporting Figure 12: ^{1}H NMR spetrum of **1** (400 MHz, $CDCl_3$, 295 K)

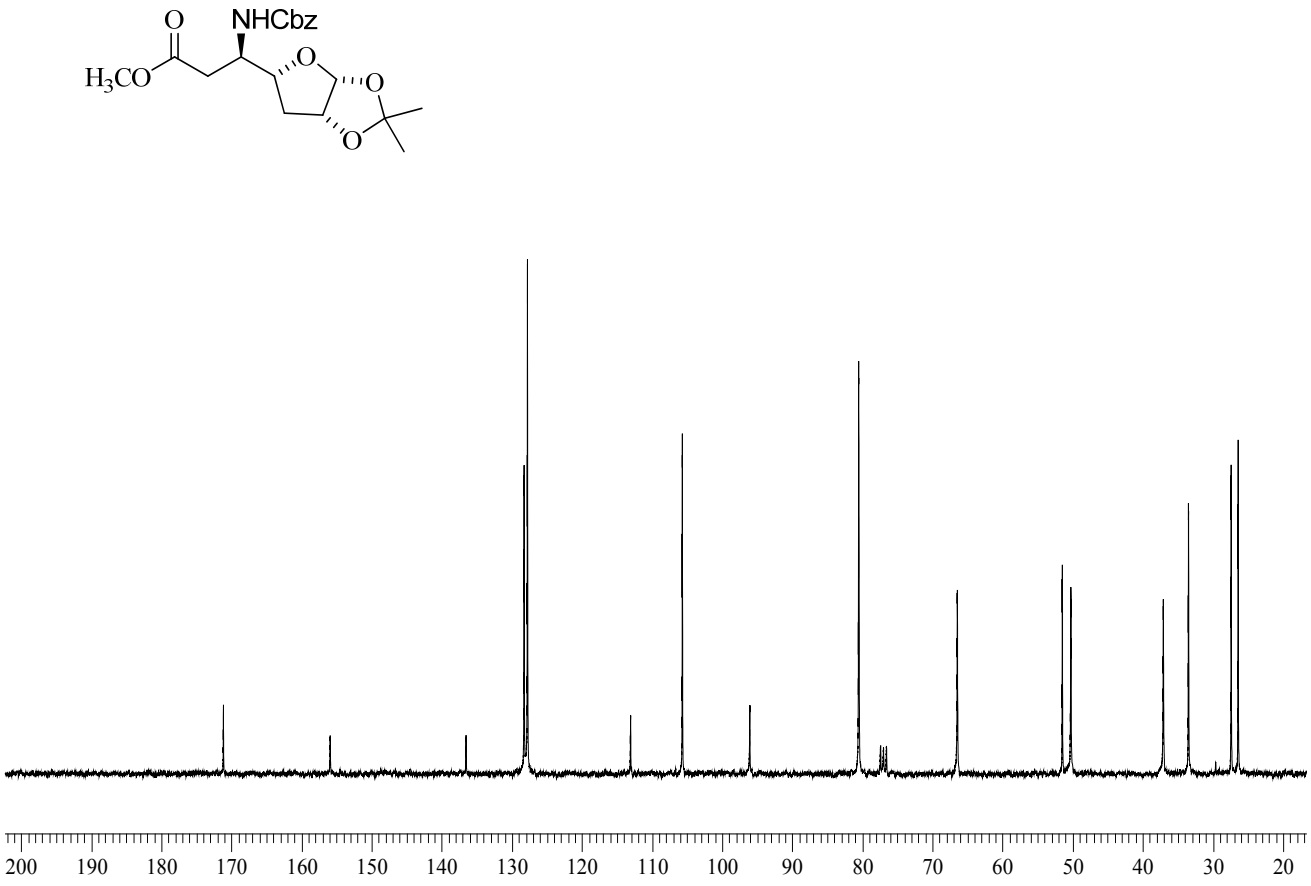

Supporting Figure 13: ^{13}C NMR spetrum of **1** (75 MHz, $CDCl_3$, 295 K)

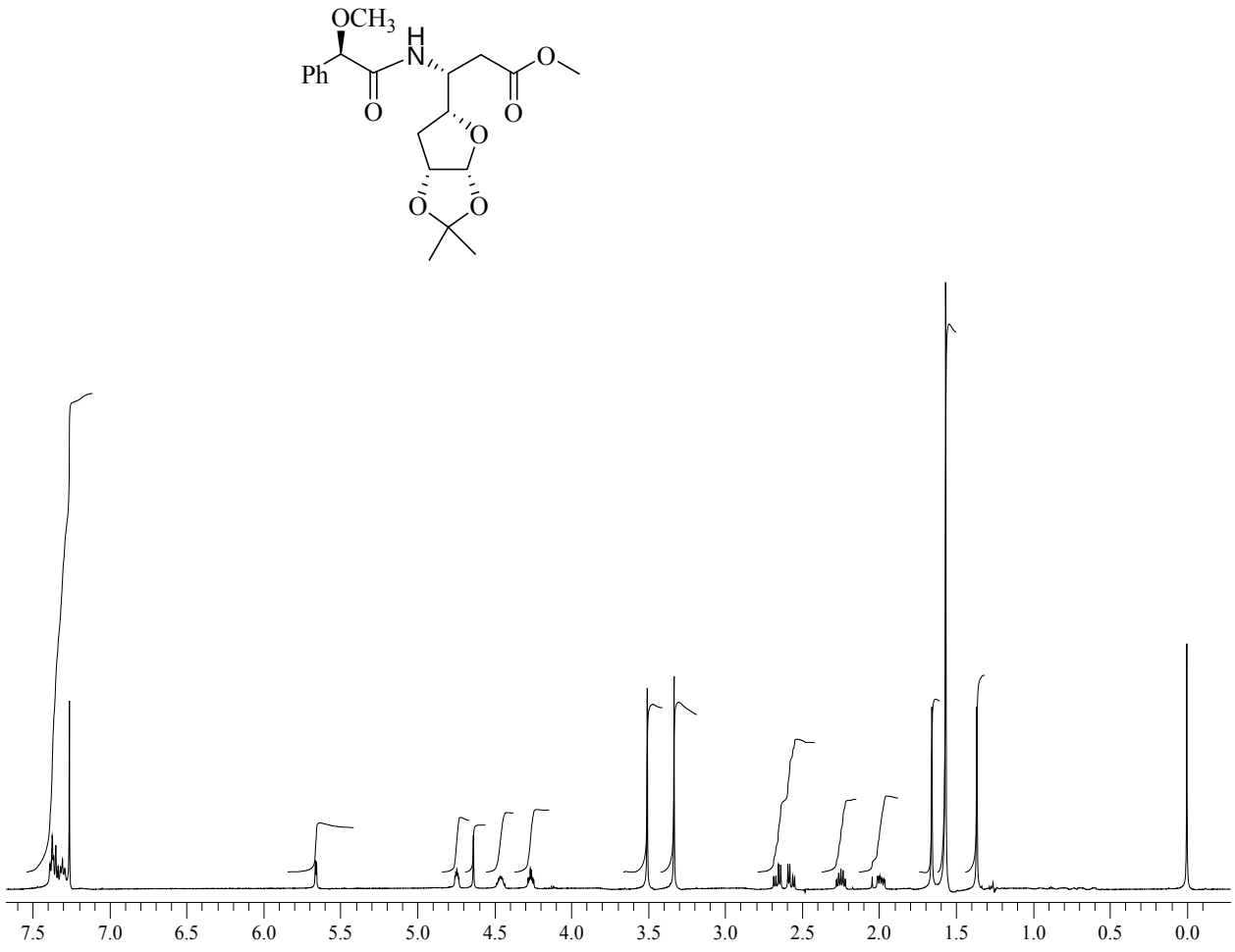

Supporting Figure 14: ^{1}H NMR spetrum of **13a** (500 MHz, $CDCl_3$, 295 K)

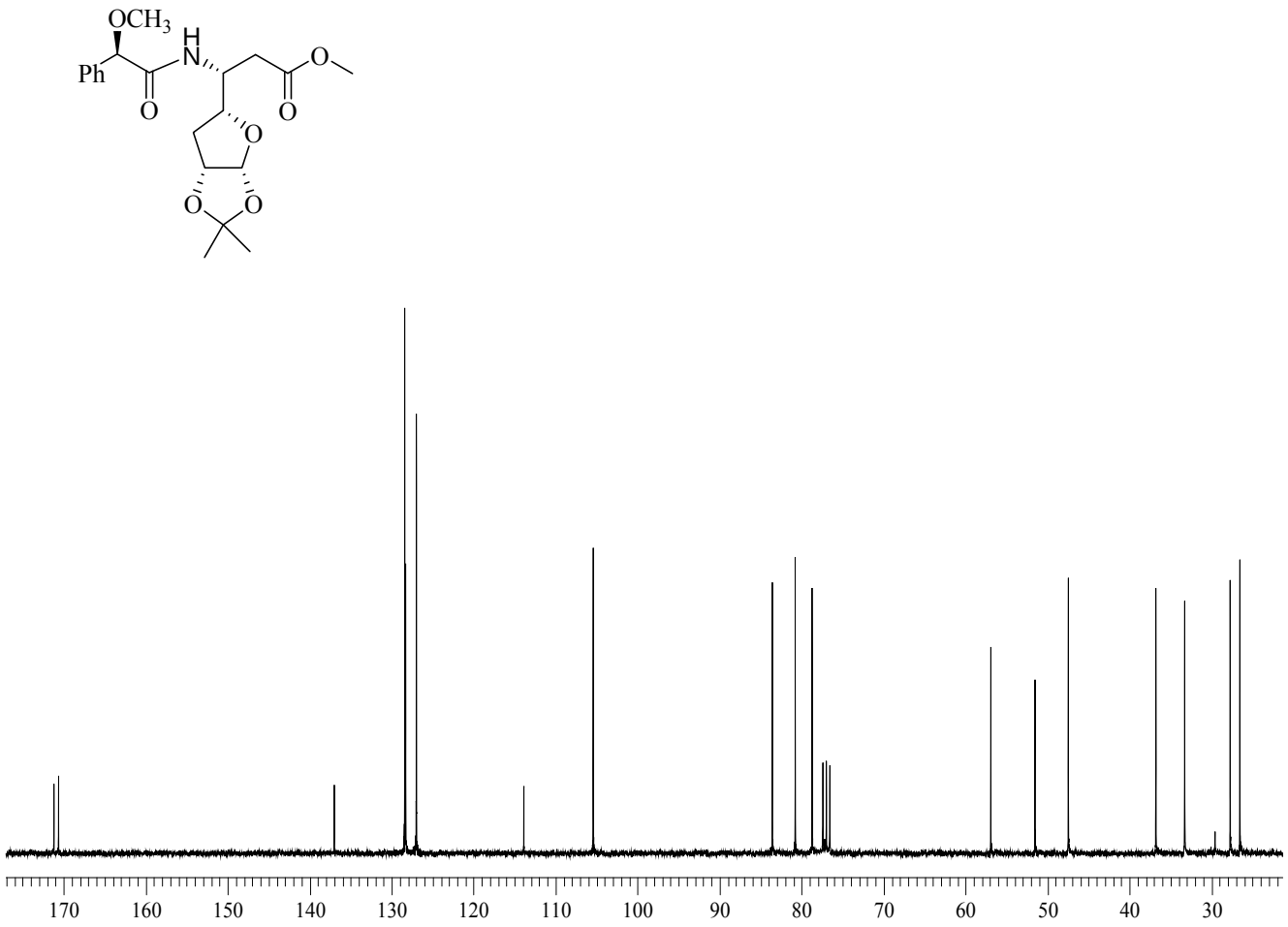

Supporting Figure 15: ^{13}C NMR spetrum of **13a** (75 MHz, $CDCl_3$, 295 K)

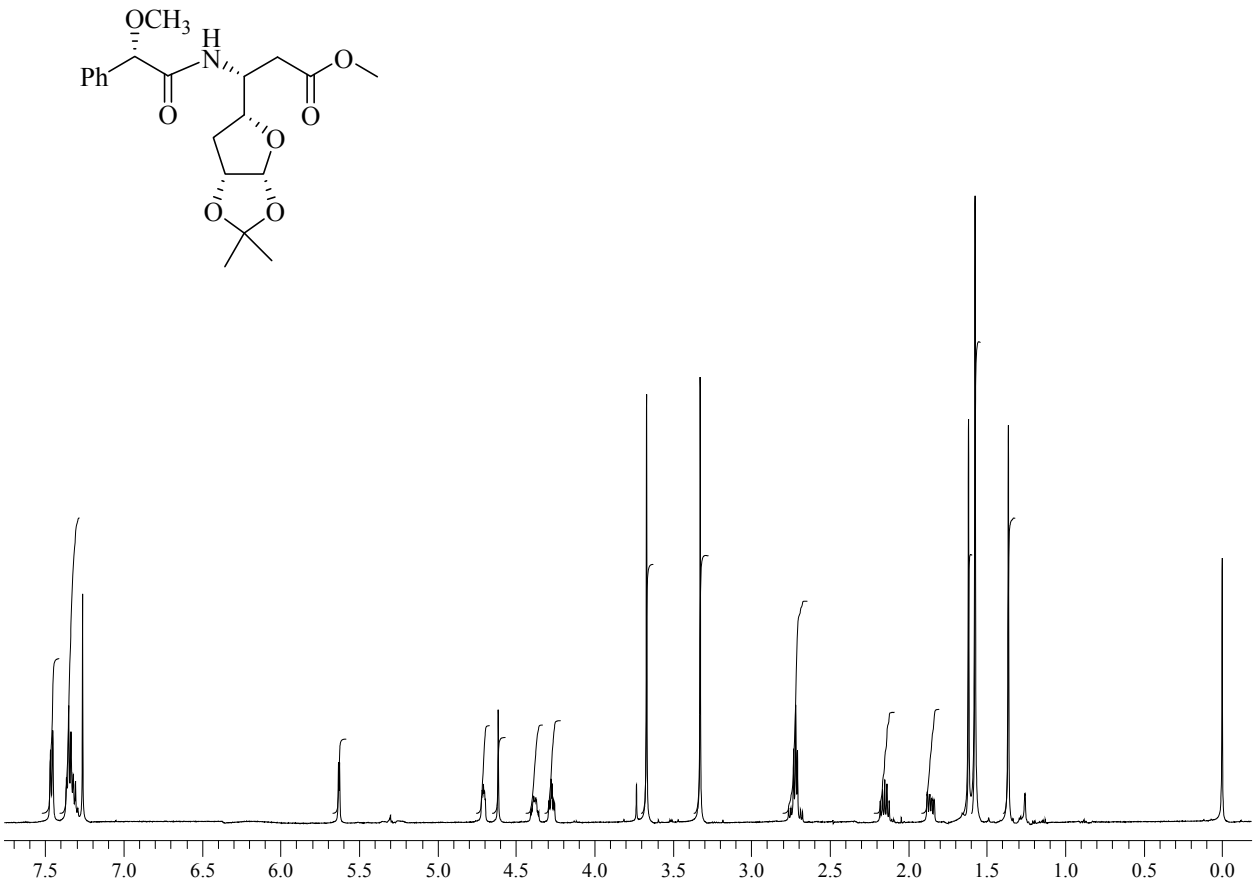

Supporting Figure 16: ^{1}H NMR spetrum of **13b** (500 MHz, $CDCl_3$, 295 K)

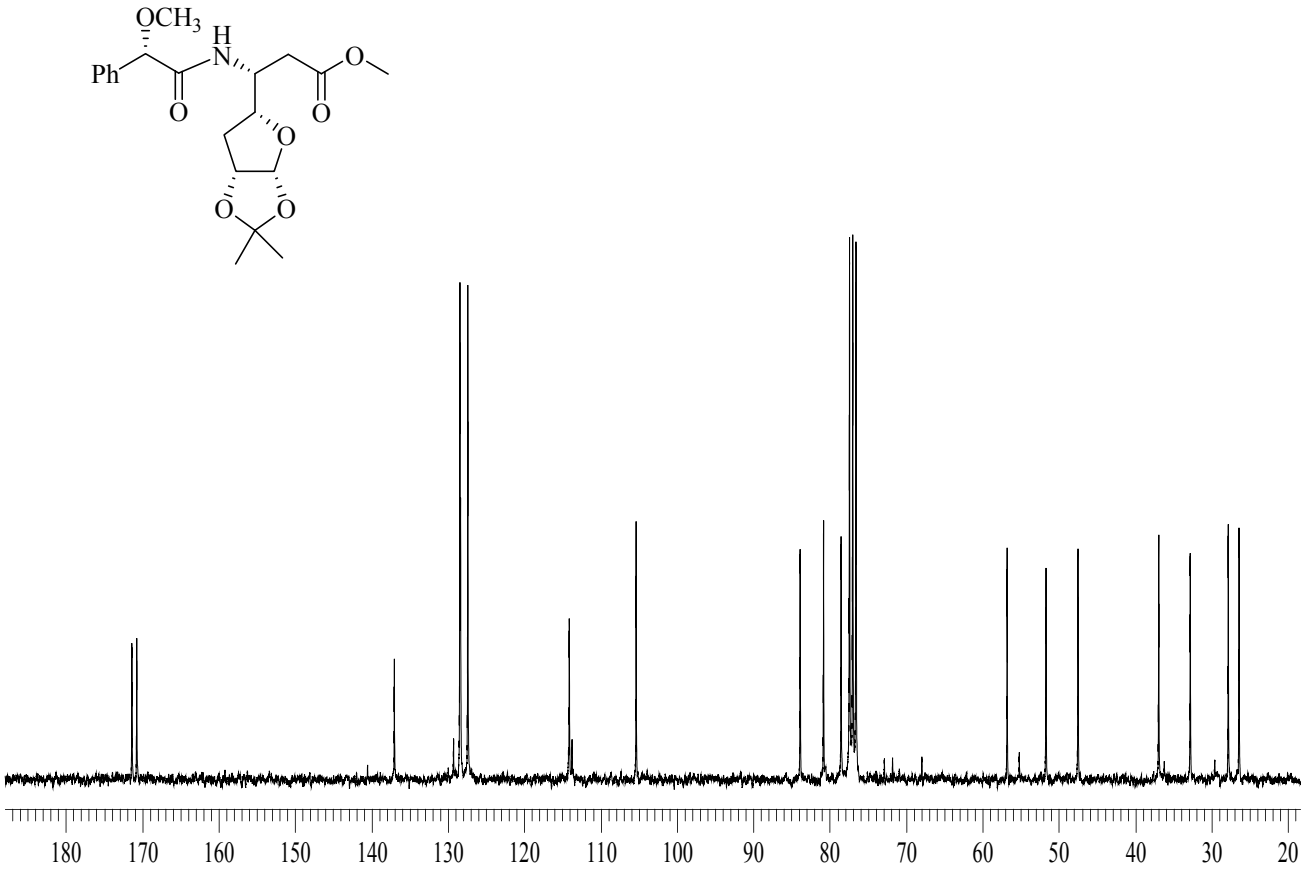

Supporting Figure 17: ^{13}C NMR spetrum of **13b** (75 MHz, $CDCl_3$, 295 K)

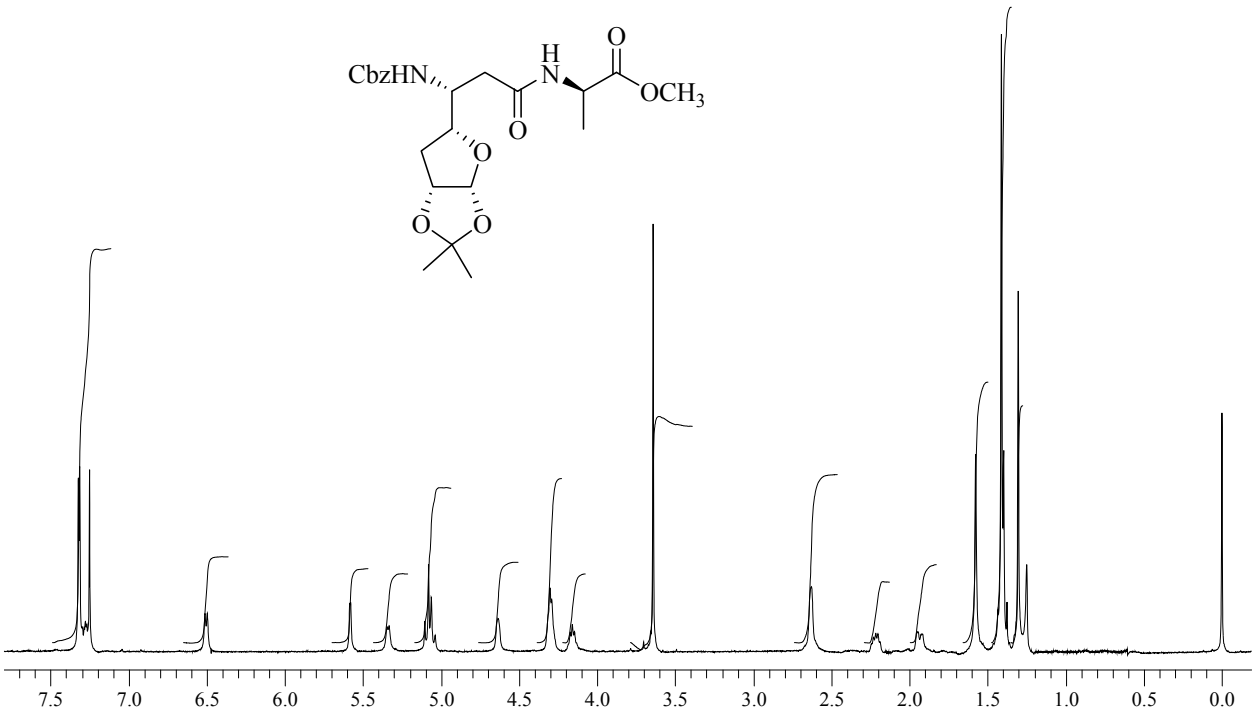

Supporting Figure 18: ^{1}H NMR spetrum of peptide **15** (500 MHz, $CDCl_3$, 295 K)

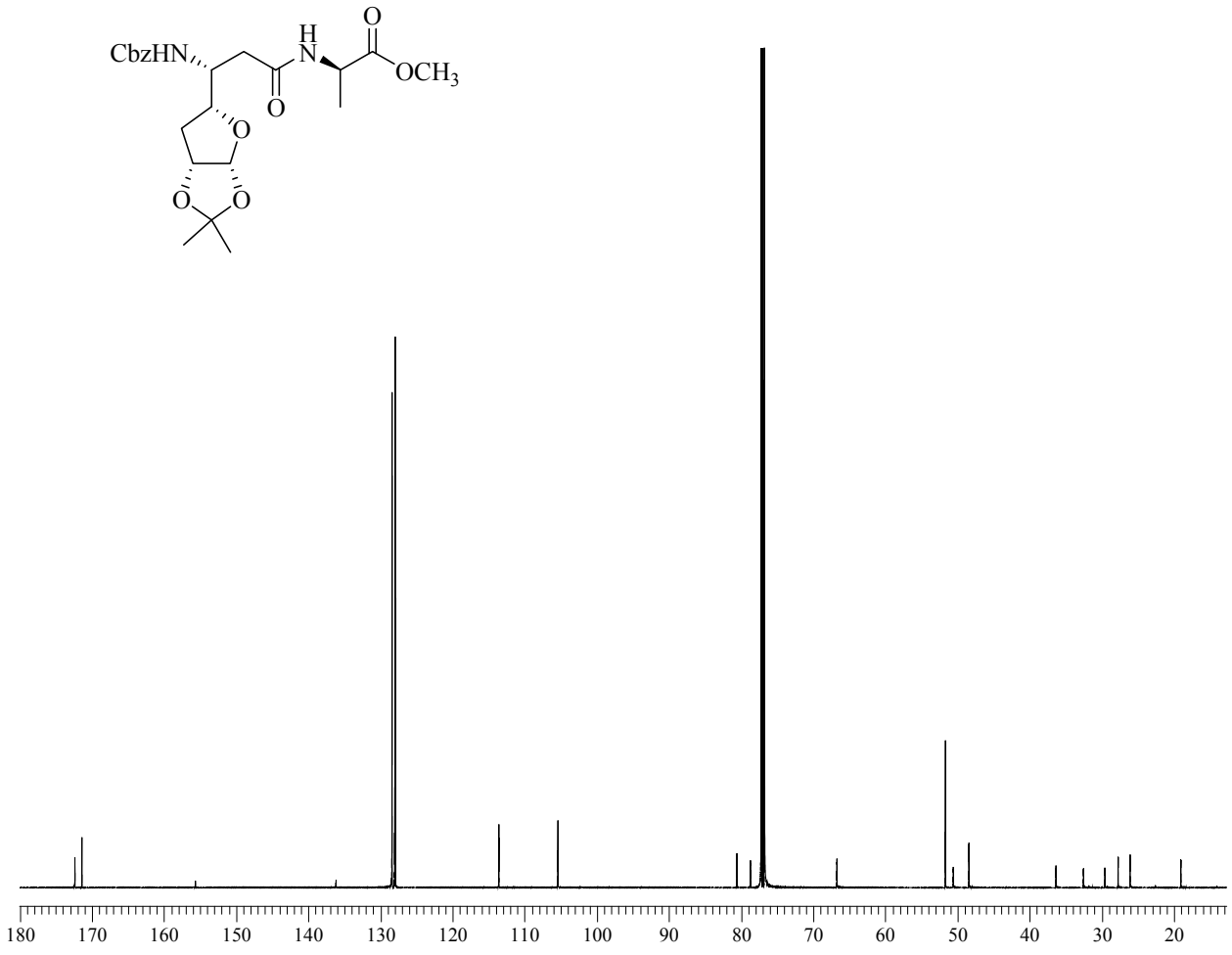

Supporting Figure 19: ^{13}C NMR spetrum of peptide **15** (75 MHz, $CDCl_3$, 295 K)

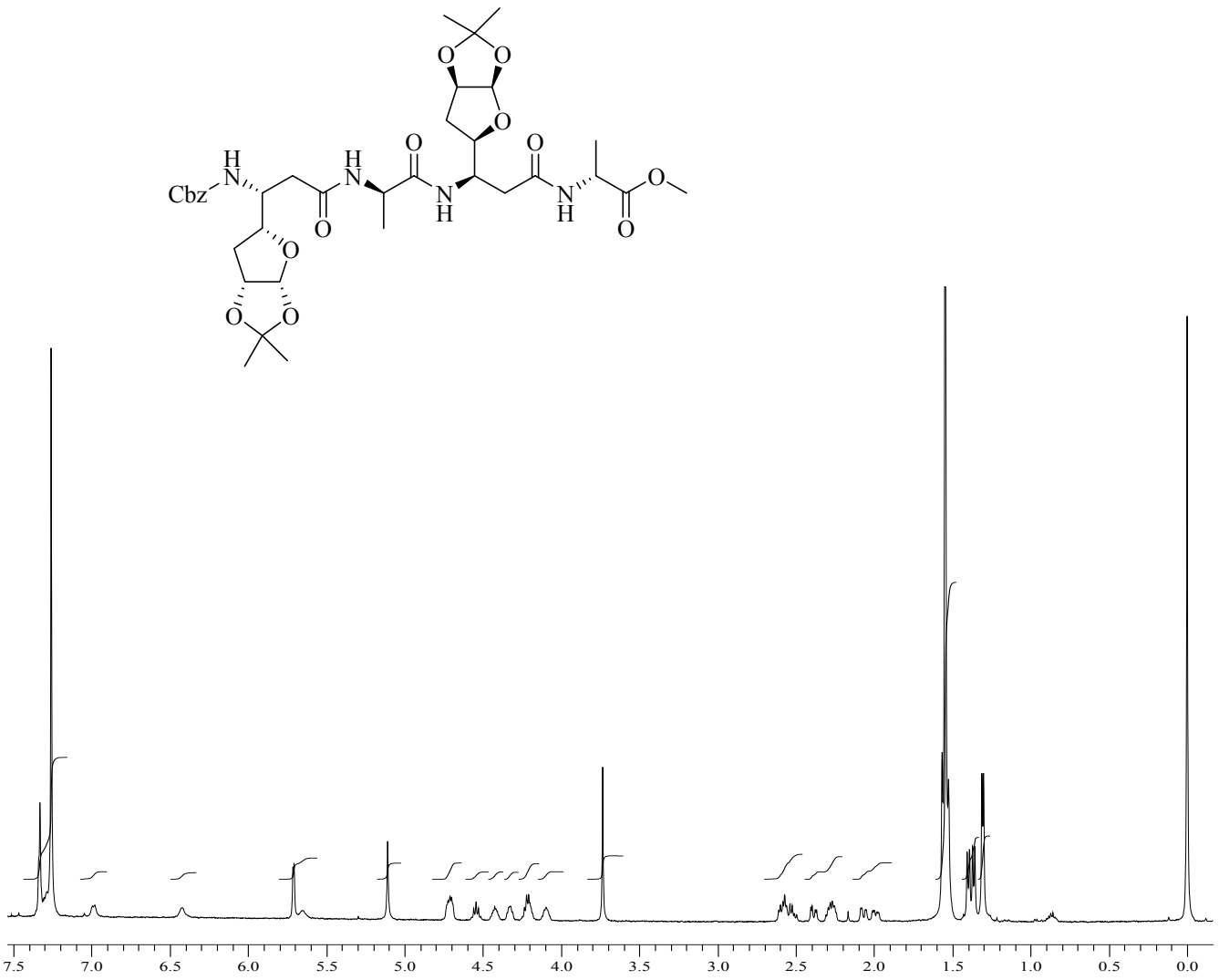

Supporting Figure 20: ^{1}H NMR spetrum of peptide **18** (500 MHz, $CDCl_3$, 295 K)

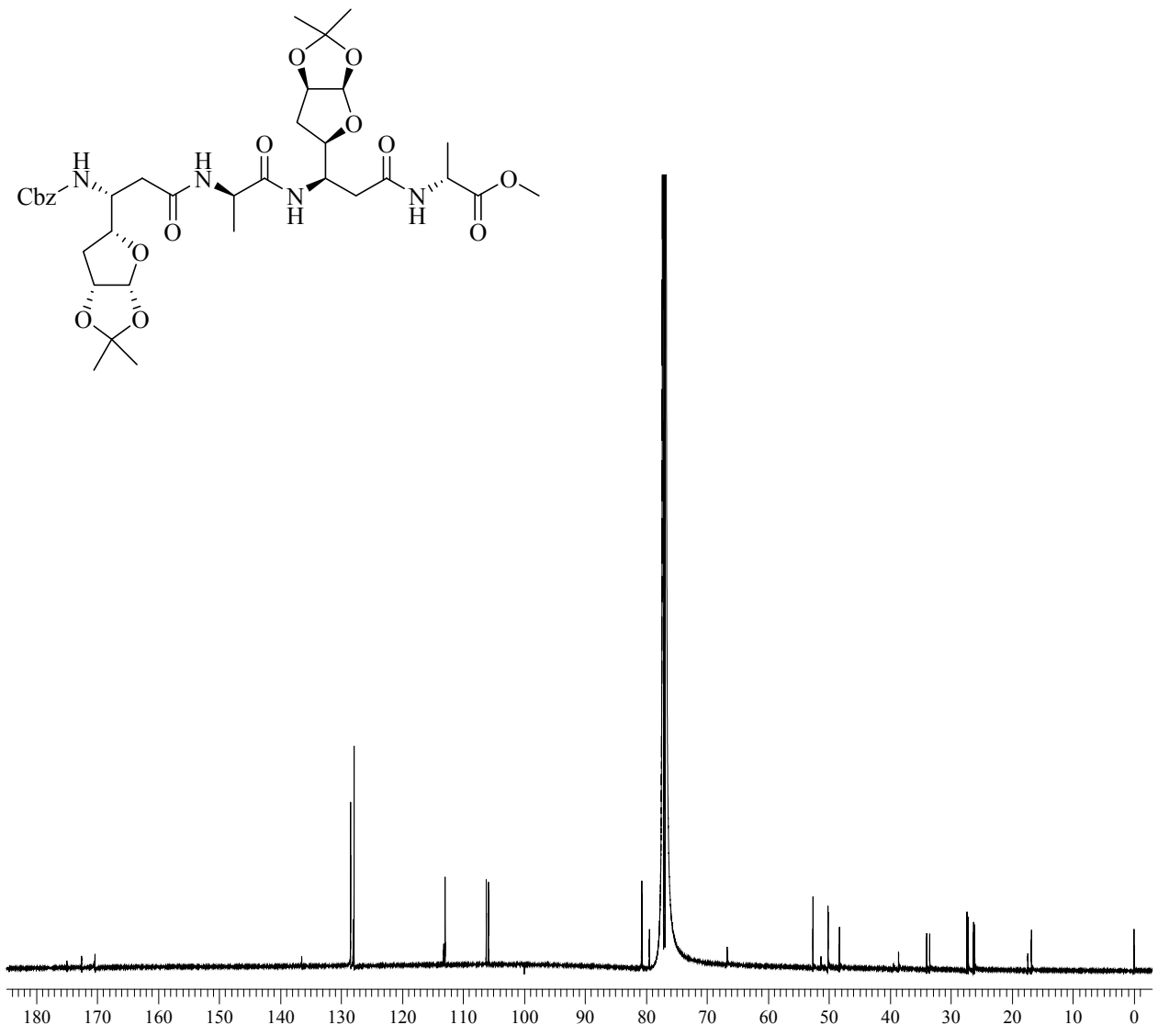

Supporting Figure 21: ^{13}C NMR spetrum of peptide **18** (150 MHz, $CDCl_3$, 295 K)

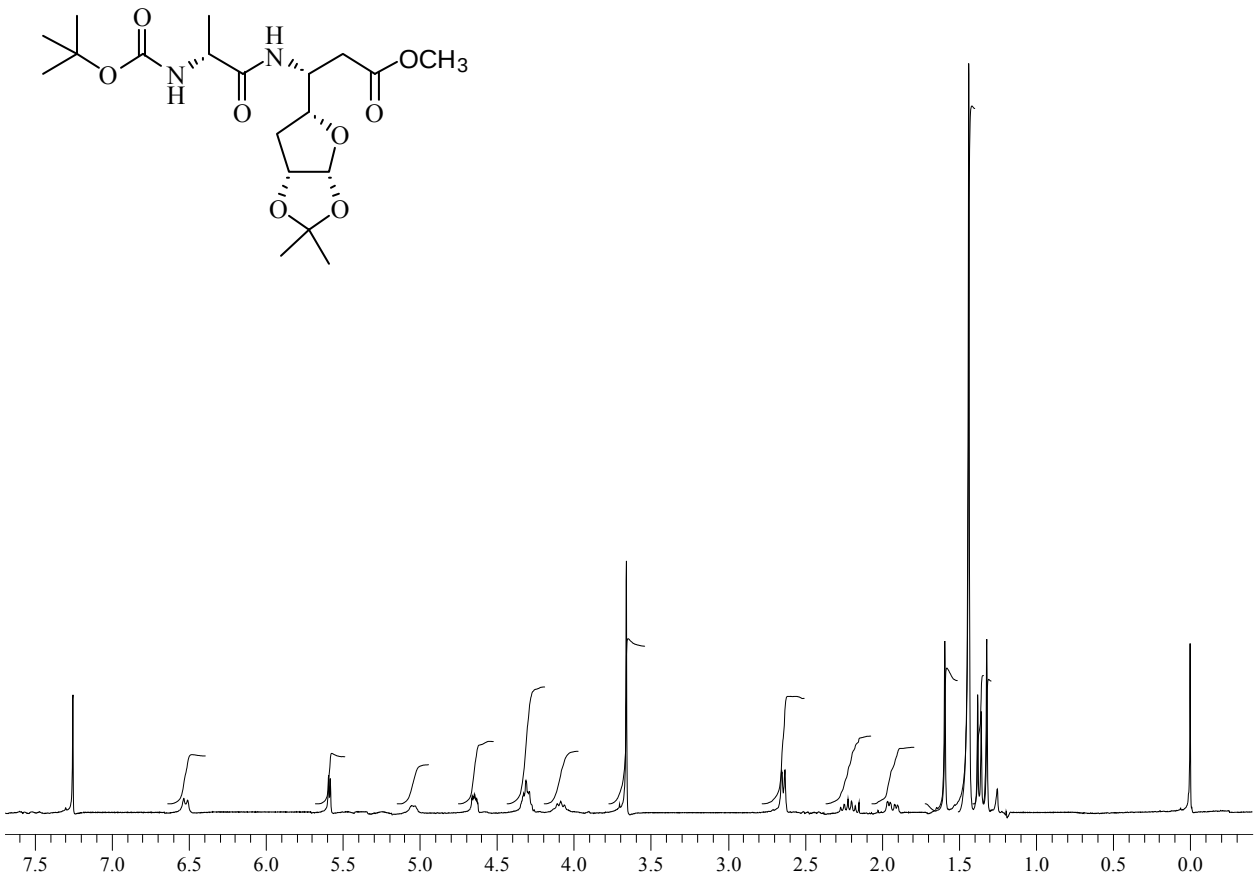

Supporting Figure 22: ^{1}H NMR spetrum of peptide **20** (300 MHz, $CDCl_3$, 295 K)

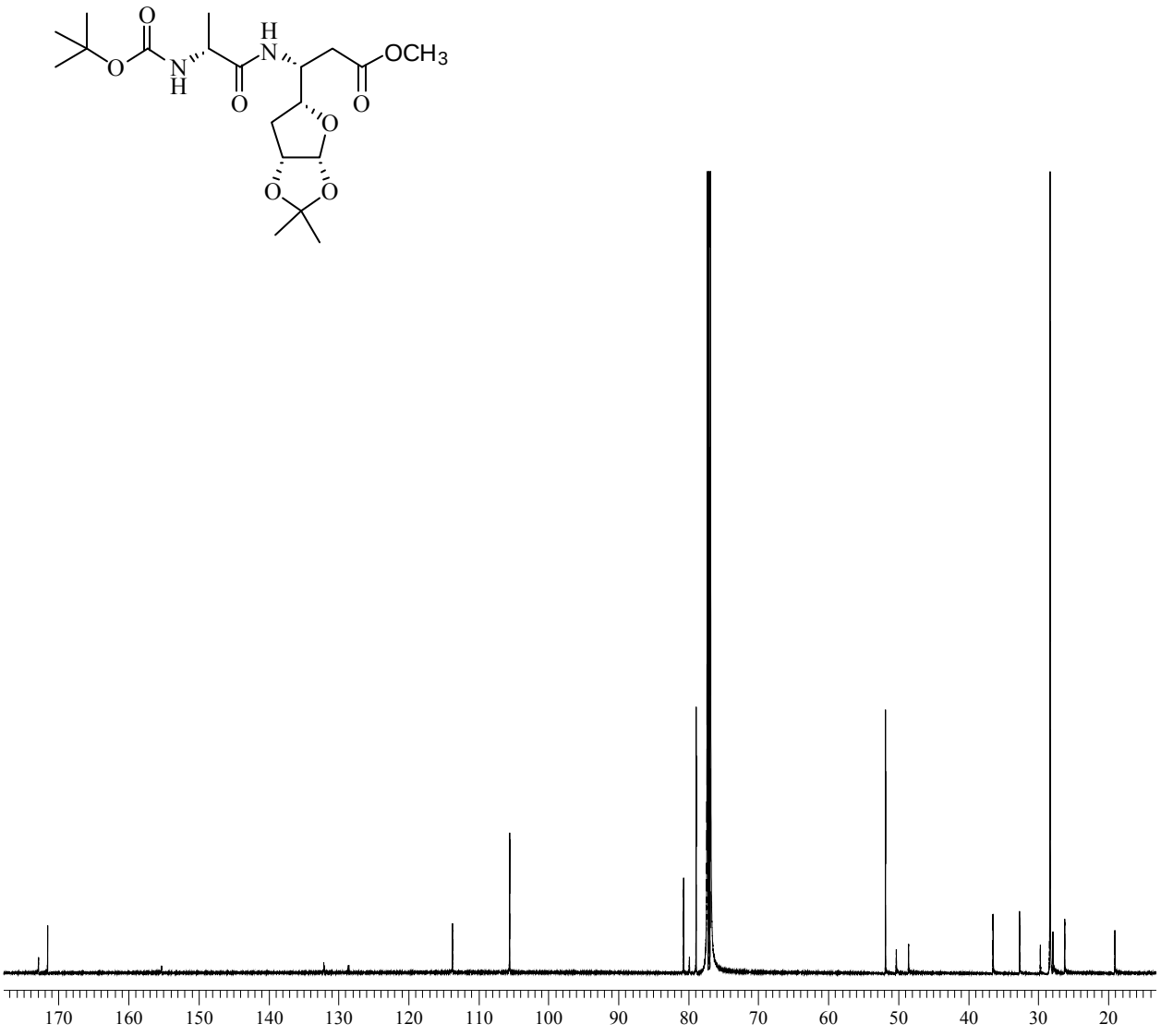

Supporting Figure 23: ^{13}C NMR spetrum of peptide **20** (75 MHz, $CDCl_3$, 295 K)

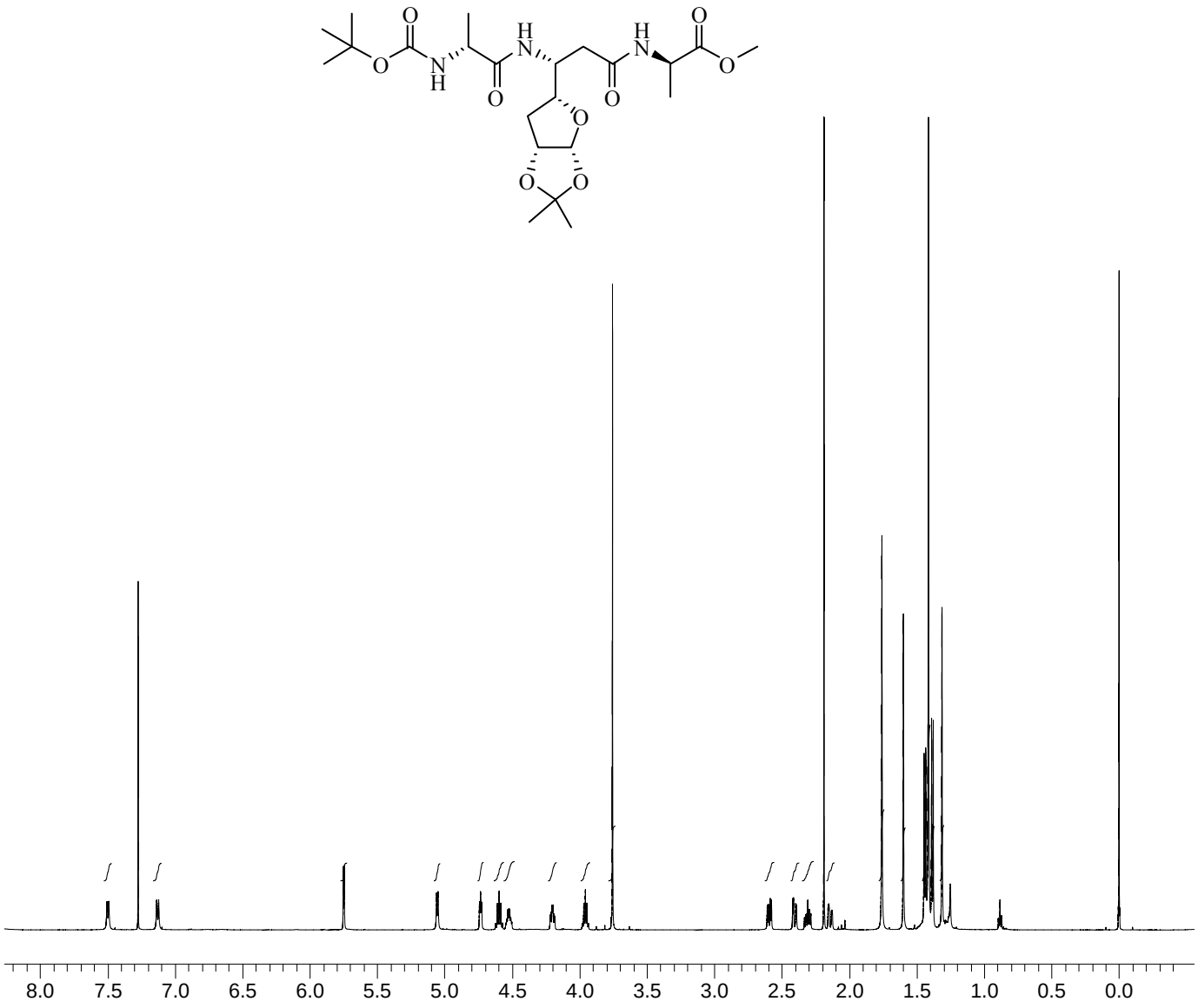

Supporting Figure 24: ^{1}H NMR spetrum of peptide **3** (600 MHz, $CDCl_3$, 288 K)

Supporting Figure 25: ^{13}C NMR spetrum of peptide **3** (150 MHz, $CDCl_3$, 295 K)

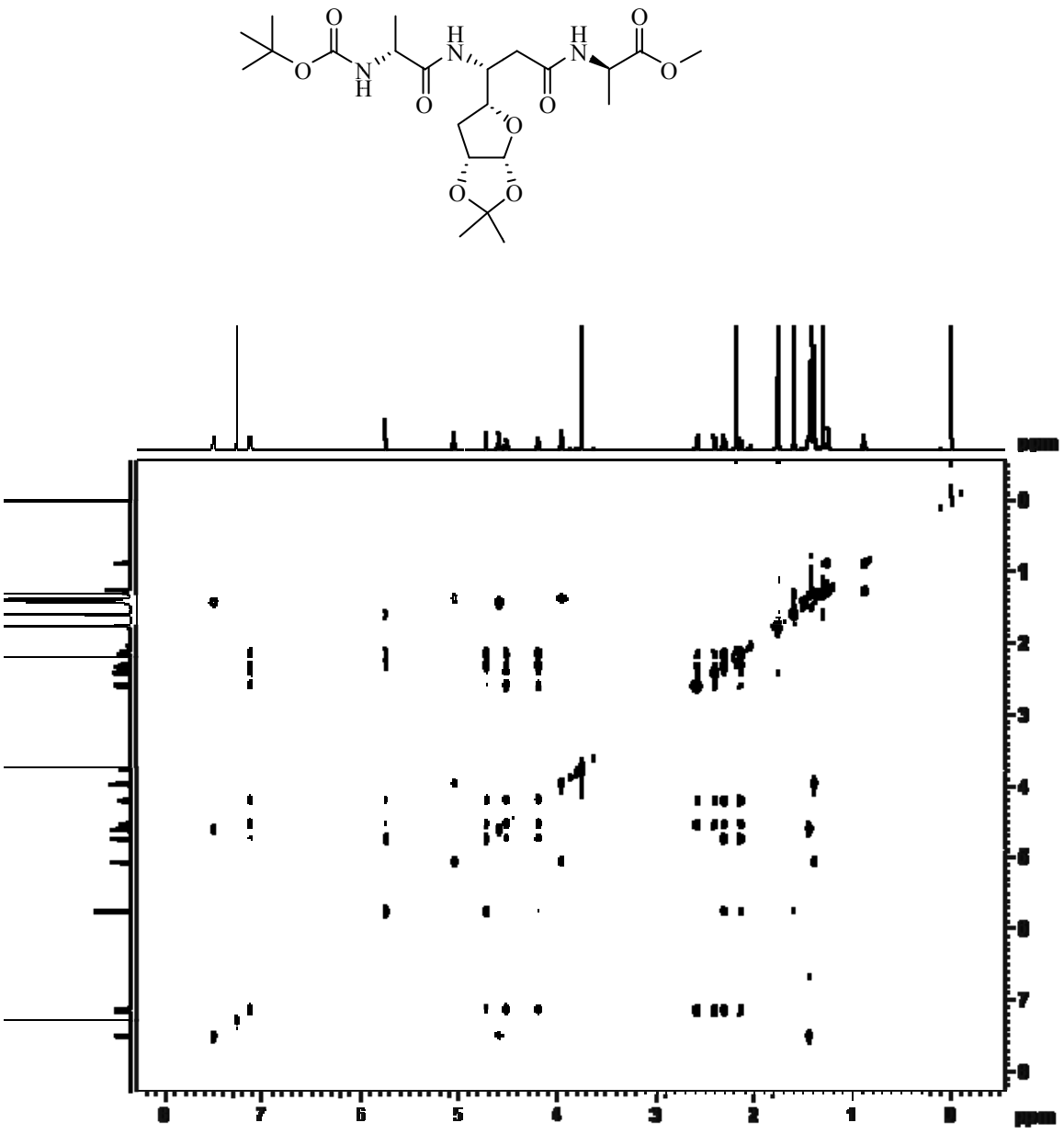

Supporting Figure 26: TOCSY Spectrum of **3** (600 MHz, $CDCl_3$, 288K).

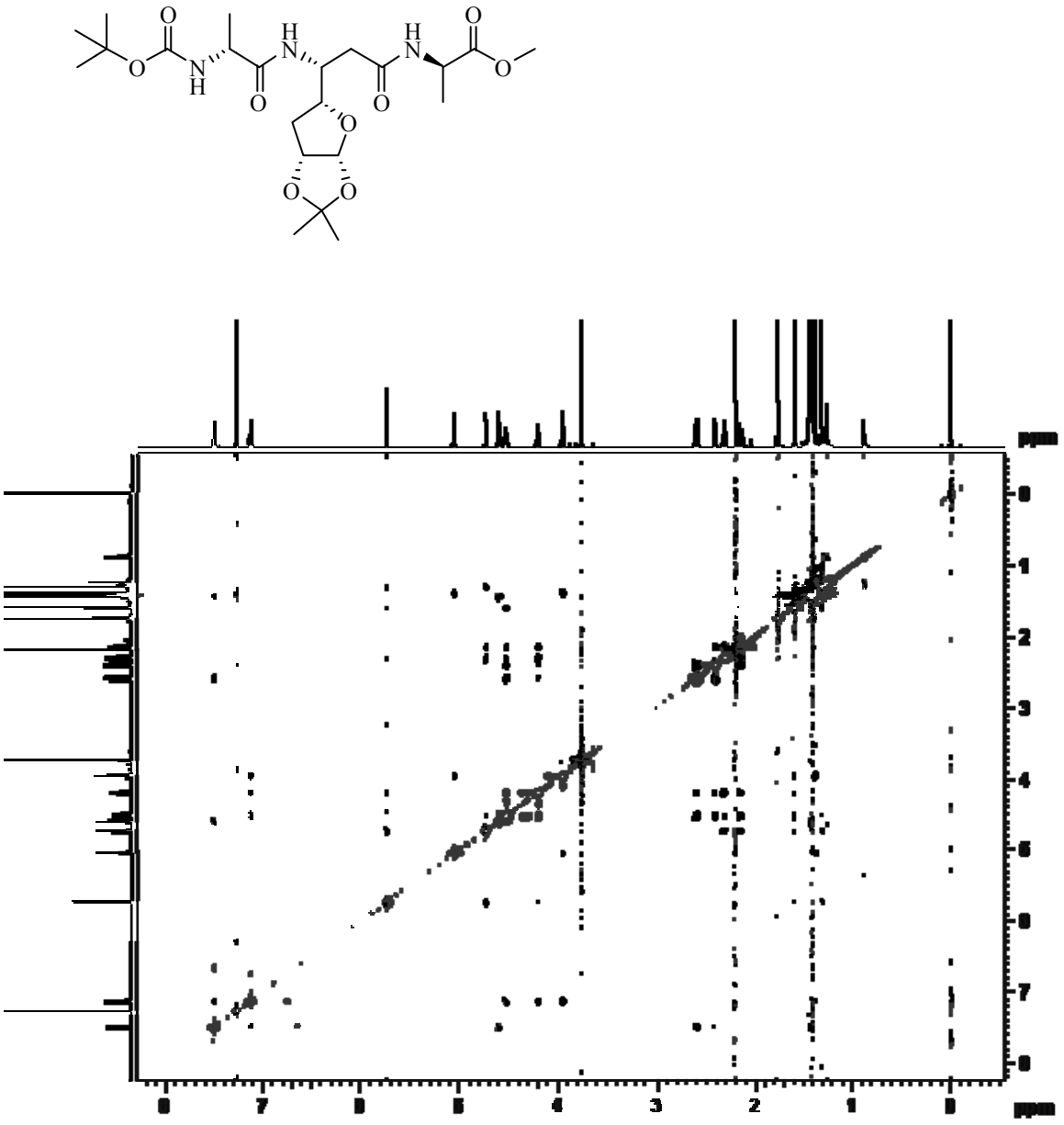

Supporting Figure 27: ROESY Spectrum of **3** (600 MHz, $CDCl_3$, 278K).

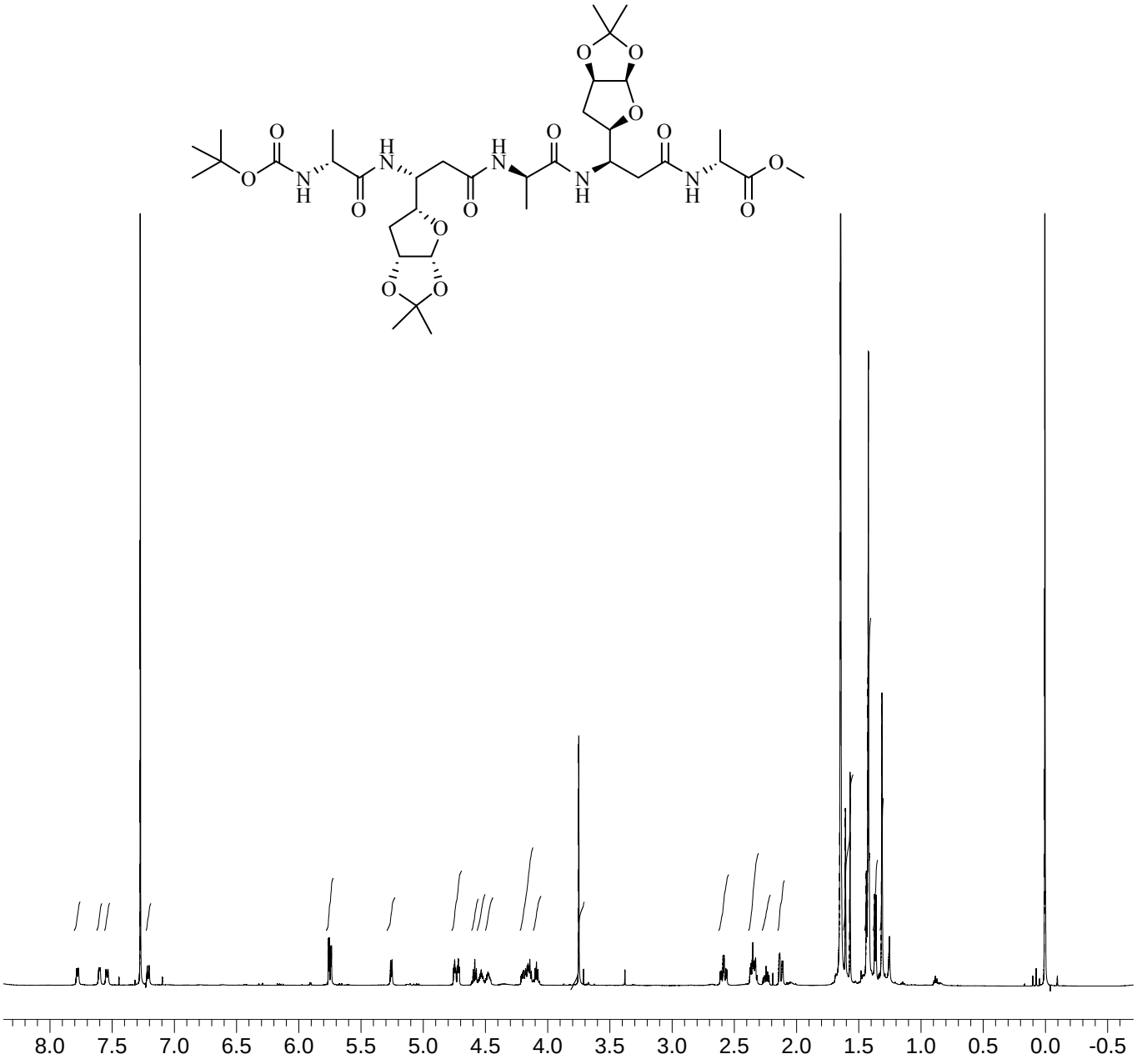

Supporting Figure 28: ^{1}H NMR spetrum of peptide **4** (600 MHz, $CDCl_3$, 298 K)

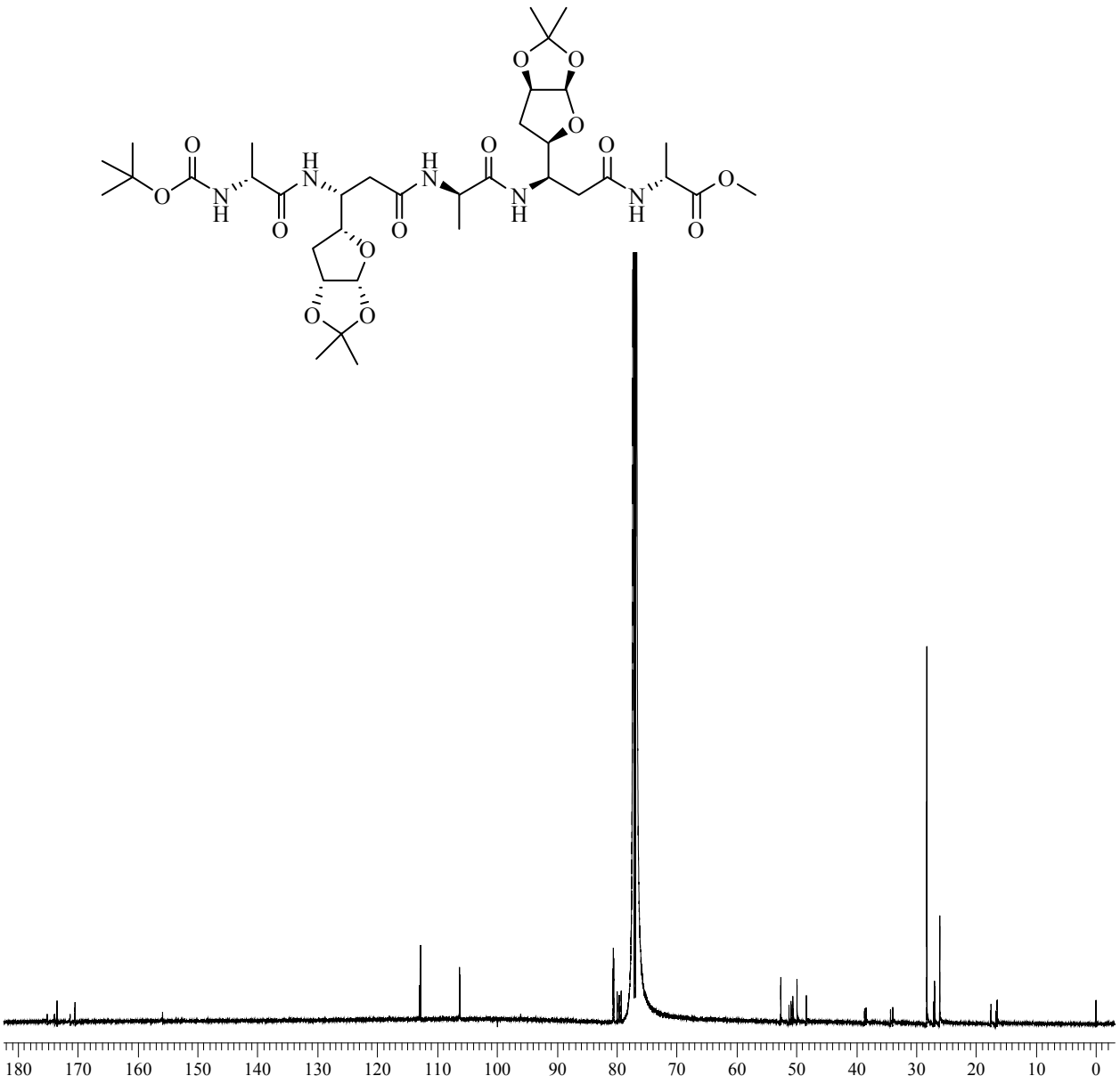

Supporting Figure 29: ^{13}C NMR spetrum of peptide **4** (150 MHz, $CDCl_3$, 295 K)

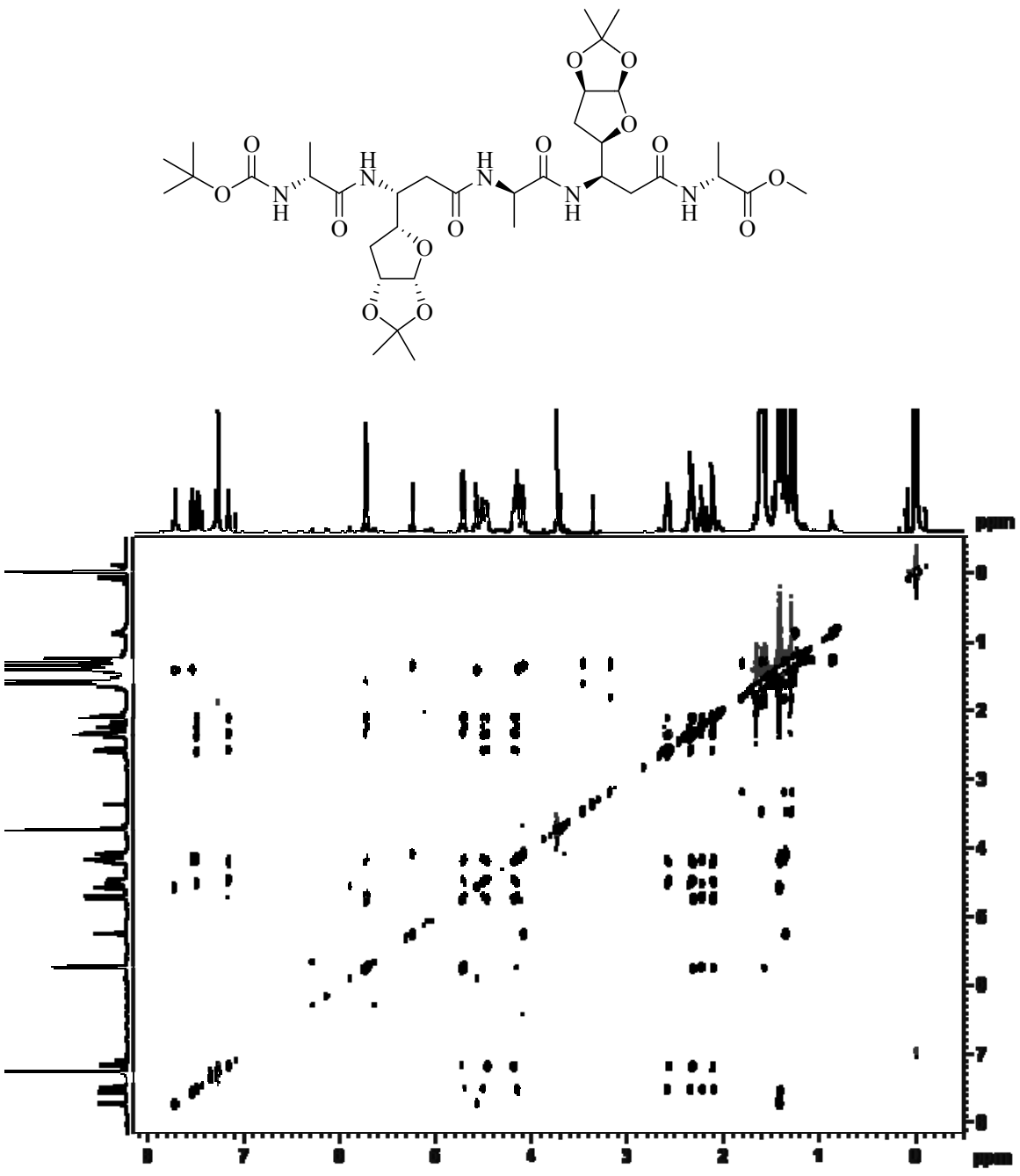

Supporting Figure 30: TOCSY Spectrum of **4** (600 MHz, $CDCl_3$, 288K).

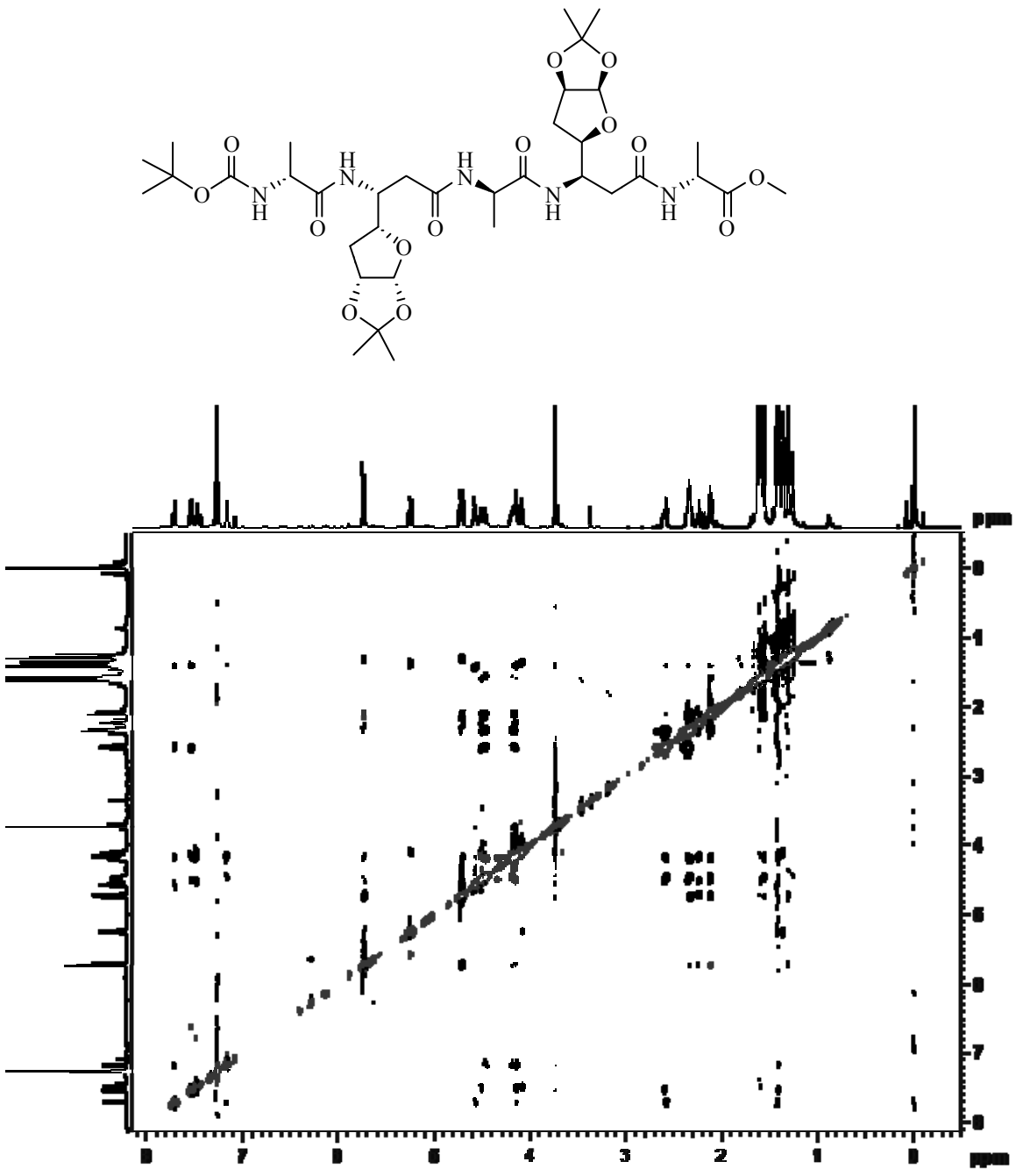

Supporting Figure 31: ROESY Spectrum of **4** (600 MHz, $CDCl_3$, 288K).

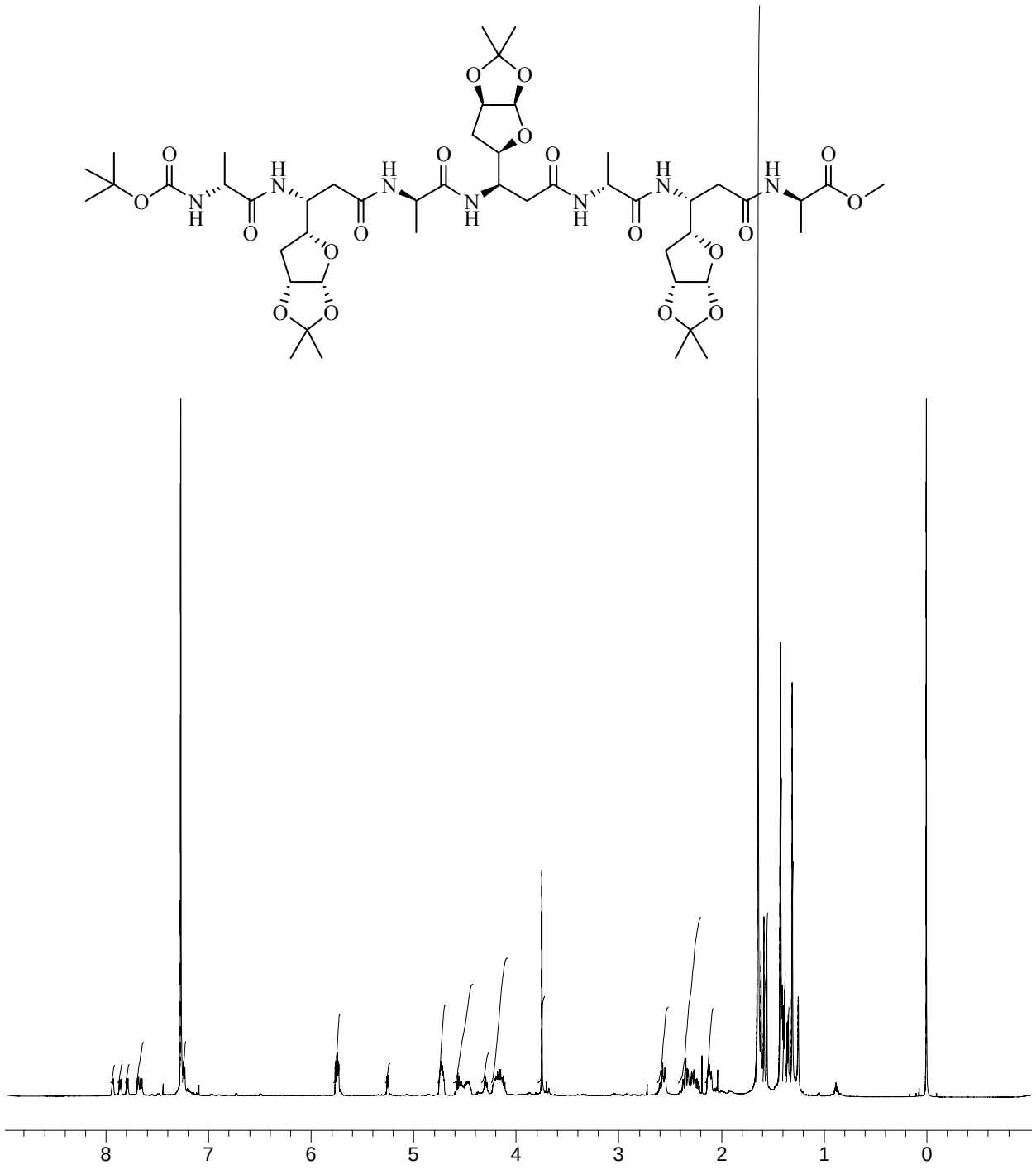

Supporting Figure 32: ^{1}H NMR spetrum of peptide **5** (500 MHz, $CDCl_3$, 288 K)

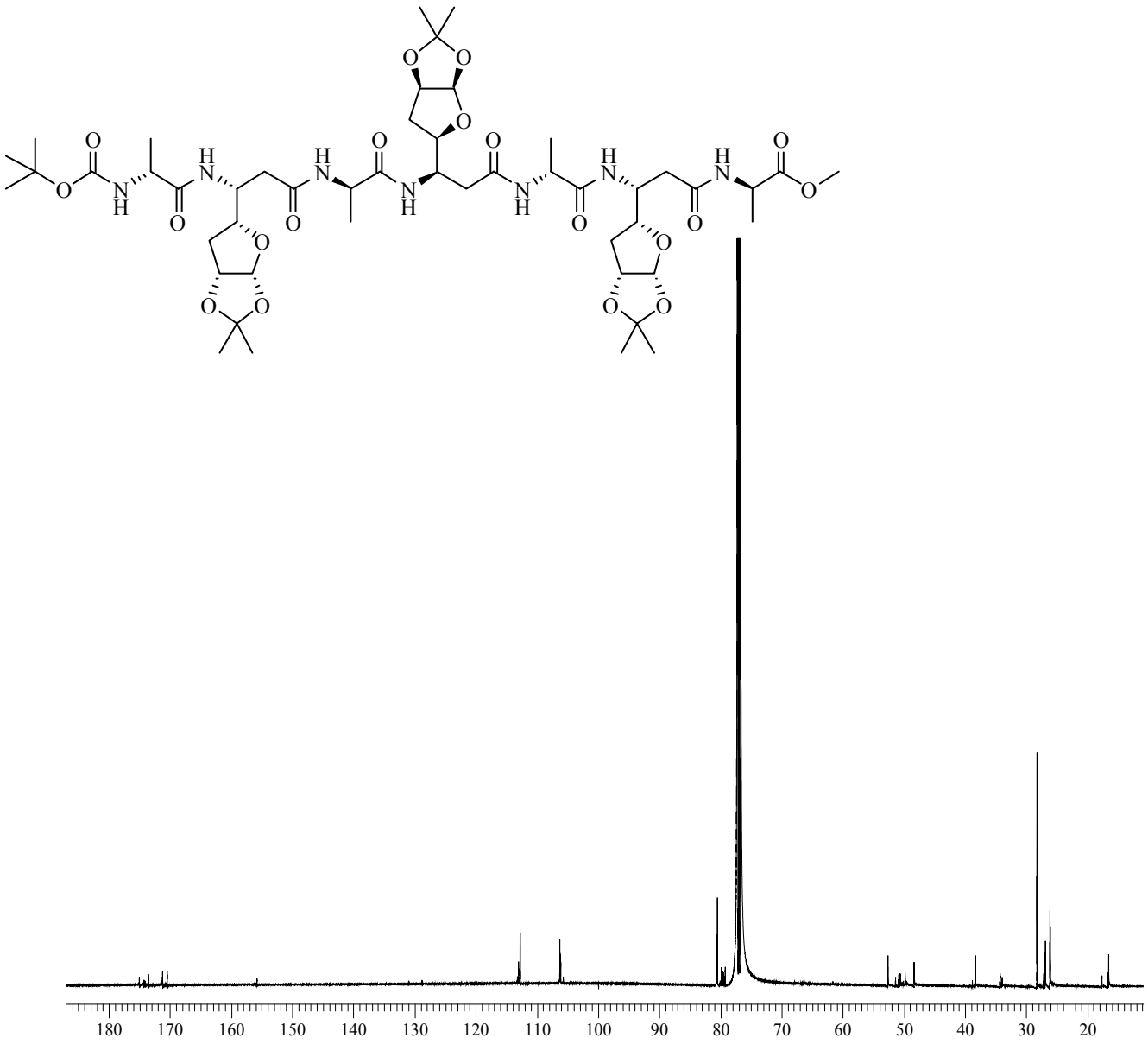

Supporting Figure 33: ^{13}C NMR spetrum of peptide **5** (150 MHz, $CDCl_3$, 295 K)

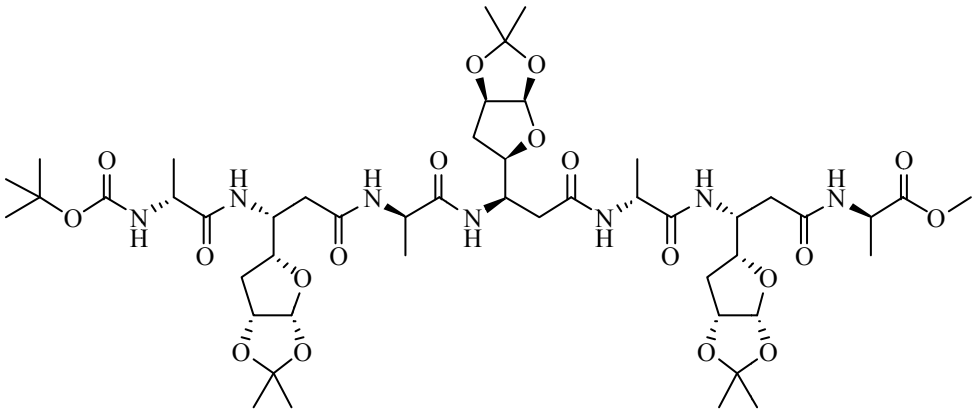

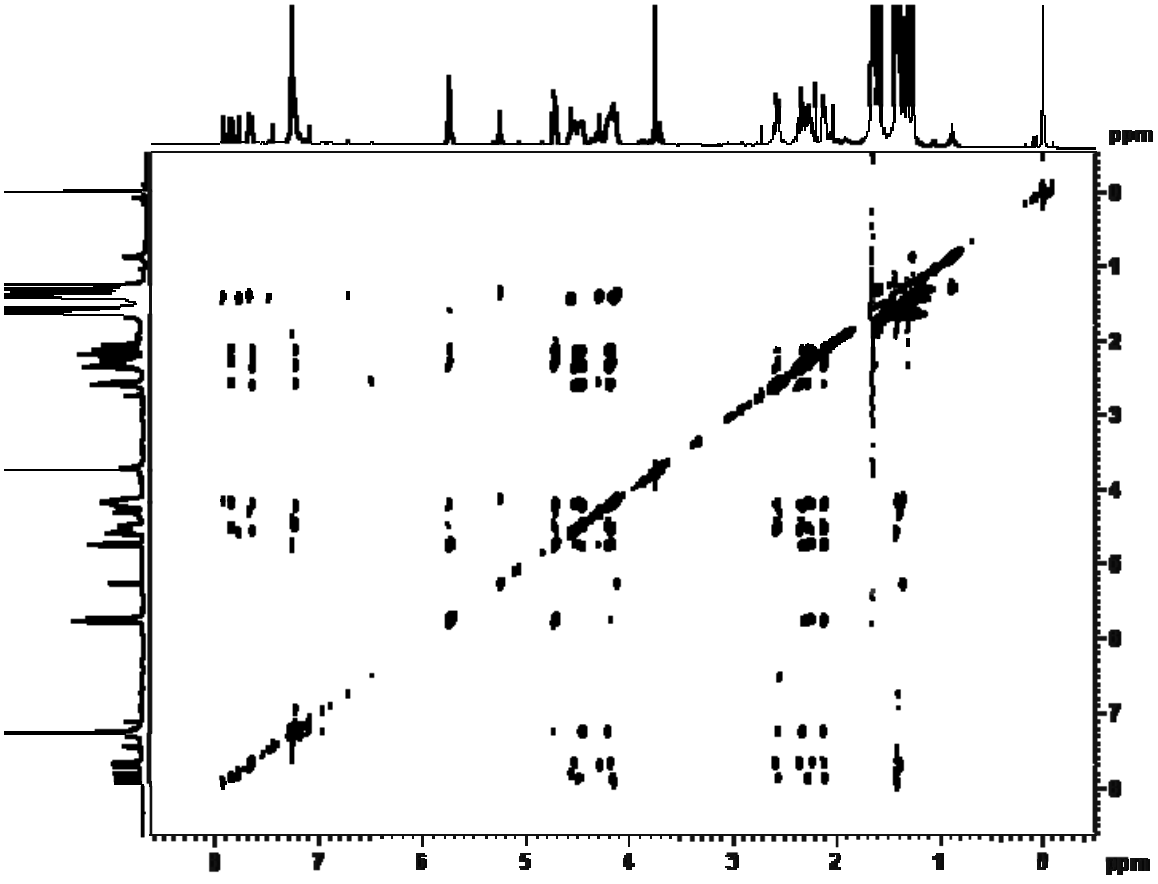

Supporting Figure 34: TOCSY Spectrum of **5** (600 MHz, $CDCl_3$, 288K).

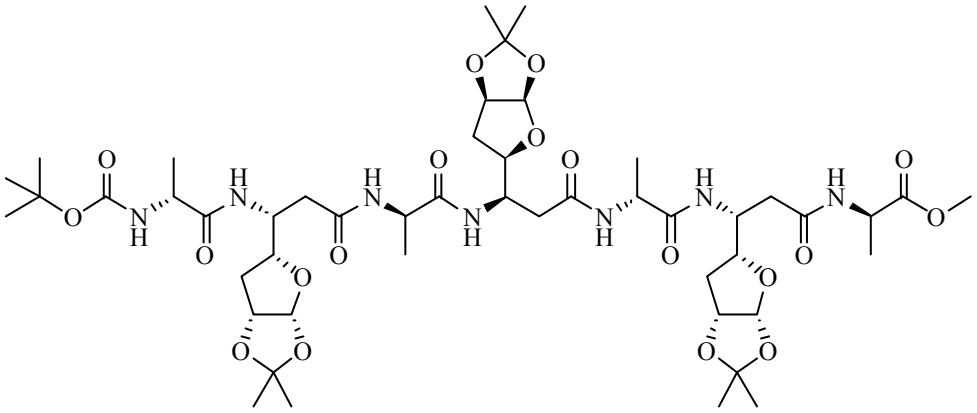

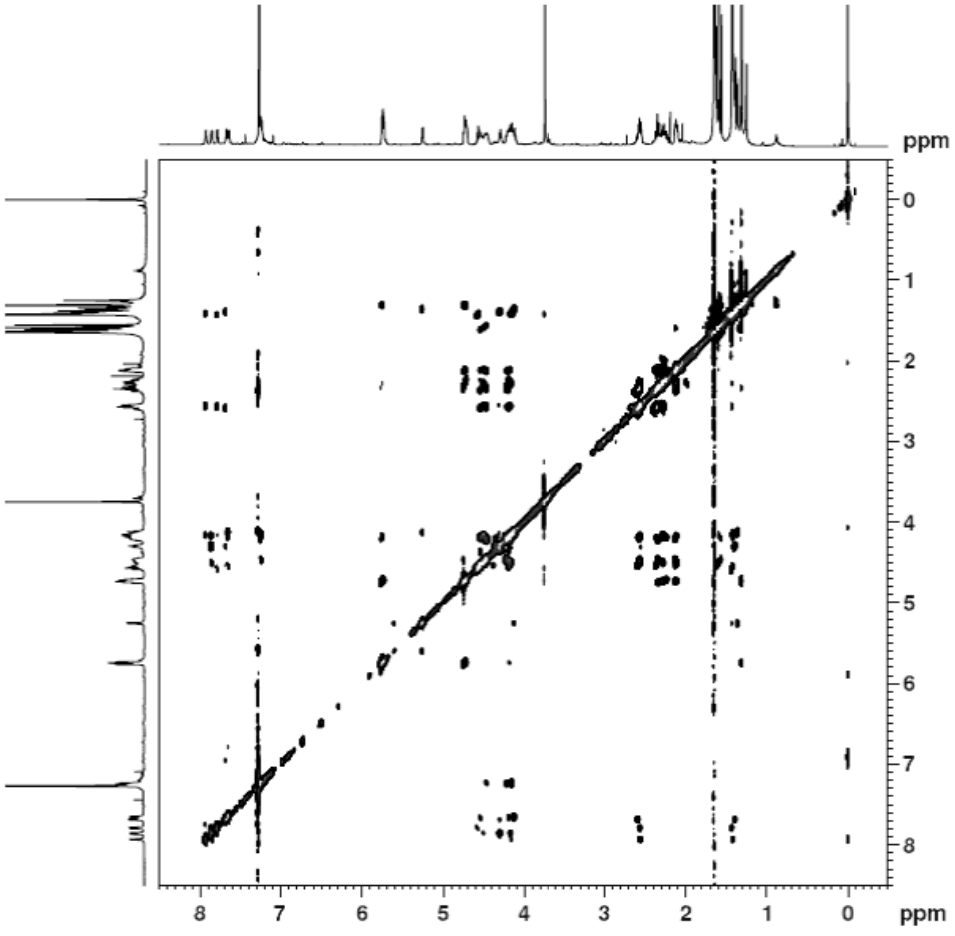

Supporting Figure 35: ROESY Spectrum of peptide **5** (600 MHz, $CDCl_3$, 288K).

Molecular Dynamics (MD): Model building and molecular dynamics simulations on peptides were carried out using the Insight II (97.0)/ Discover program on a Silicon Graphics O2 workstation. The CVFF MSI version with default parameter was used as force field throughout the calculation using a distance dependent dielectric constant with $\varepsilon = 4.7$ (dielectric constant of deuterated chloroform). The constraints were derived from the volume integrals obtained from the ROESY spectra using a two-spin approximation and a reference distance of 1.8 Å for the geminal protons $C_\alpha H$ and $C_{\alpha'} H$ .The upper and lower bound of the distance constraints have been obtained by enhancing and reducing the derived distance by 10%. The dihedral angles ϕ_β and θ_β were constrained around - 120° ± 30° and - 60° ± 30°. The couplings, $^3J_{NH\text{-}C\beta H}$ are however quite distinctive, with large values (> 8.9 Hz), which correspond to $\phi_\beta \sim$ - 120°. The complete set of nOe distance constraints used for structure calculation is shown in supporting information as a first step, a mild minimization with constraints was performed in order to remove bad steric contacts and improve the stability of the calculations. The following general protocol was used for minimizing energy. Each structure was energy minimized by steepest descent method, followed by conjugate gradient method for a maximum of 1000 iterations each or RMS deviation of 0.001 kcal/mol, whichever was earlier. For MD runs, a temperature of 300 K was used. The molecules were initially equilibrated for 50 ps and subsequently subjected to an 2 ns dynamics with a step size of 1 fs, sampling the trajectory at equal intervals of 20 ps. In this trajectory, 100 samples were generated and were again energy minimized. For MD runs, a temperature of 300 K was used. In this trajectory, 100 samples were generated and were again energy minimized. Discover Studio 3.5 program was used for RMSD calculations and alignment of different conformations.

Supporting Table 2: Distance constraints used in the MD calculations for 4.

Residue	Atom	Residue	Atom	Upper Bound	Lower Bound
1	CαH	2	NH	2.52	2.06
2	NH	2	C4H	2.85	2.33
2	NH	2	$C\alpha H_{(pro\text{-}S)}$	4.60	3.84
2	$C\alpha H_{(pro\text{-}R)}$	2	C4H	3.16	2.58
2	$C\alpha H_{(pro\text{-}S)}$	3	NH	2.08	2.54
2	CβH	3	NH	3.60	2.94
2	C4H	3	NH	4.41	3.69
3	$C\alpha H_{(pro\text{-}S)}$	4	NH	2.49	2.04
3	CαH	5	NH	3.52	2.88
4	NH	4	$C\alpha H_{(pro\text{-}S)}$	4.05	3.32
4	NH	4	C4H	2.81	2.30
4	$C\alpha H_{(pro\text{-}S)}$	5	NH	2.60	2.14
4	$C\alpha H_{(pro\text{-}R)}$	4	C4H	2.78	2.28
4	CβH	5	NH	4.05	3.31
4	NH	5	NH	3.50	2.86
4	C4H	5	NH	4.35	3.56

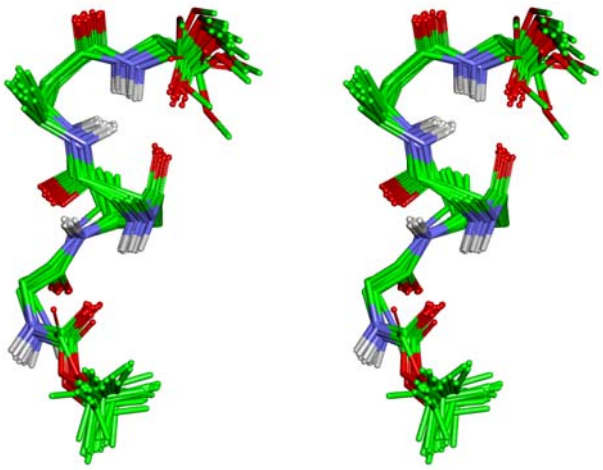

Supporting Figure 36: Stereoview of the superimposition of the 20 lowest-energy structures for **4** (for clarity, sugars are replaced with methyl groups after the calculations).

Supporting Table 3: Distance constraints used in the MD calculations for 5.

Residue	Atom	Residue	Atom	Upper Bound	Lower Bound
1	CαH	2	NH	2.66	2.17
1	CαH	3	NH	3.48	2.85
2	NH	2	C4H	3.05	2.49
2	NH	2	$C\alpha H_{(pro\text{-}S)}$	3.96	3.24
2	NH	2	C3H	4.79	3.92
2	$C\alpha H_{(pro\text{-}S)}$	3	NH	2.83	2.31
2	CβH	3	NH	3.55	2.91
3	CαH	5	NH	3.03	3.70
4	NH	4	C4H	2.81	2.42
4	NH	4	$C\alpha H_{(pro\text{-}S)}$	3.80	3.11
4	$C\alpha H_{(pro\text{-}S)}$	5	NH	2.91	2.38
4	CβH	5	NH	3.71	3.03
5	CαH	6	NH	2.44	2.01
5	CαH	7	NH	3.47	2.84
6	NH	6	C4H	2.84	2.32
6	NH	6	$C\alpha H_{(pro\text{-}S)}$	3.95	3.23
6	CαH	7	NH	2.82	2.30
6	NH	7	NH	3.60	2.94

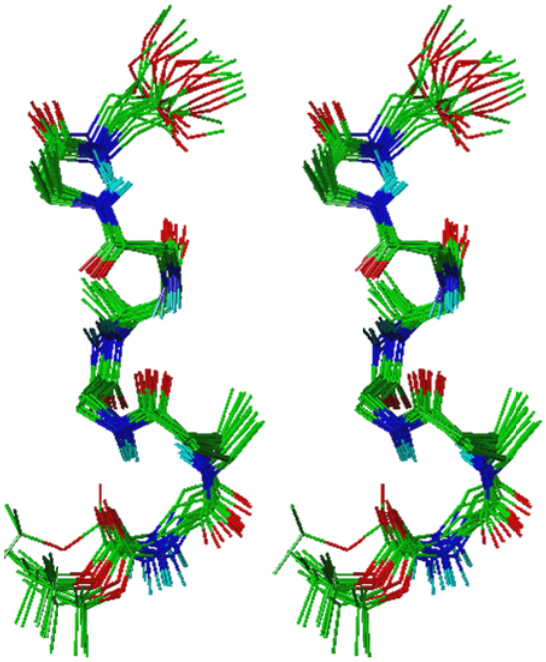

Supporting Figure 37: Stereoview of the superimposition of the 20 lowest-energy structures for **5** (for clarity, sugars are replaced with methyl groups after the calculations).

Circular Dichroism (CD):

CD spectra were obtained on a Jasco J-810 spectropolarimeter (Jasco Spectroscopic Co., Hachioji City, Japan), with a Jasco PTC-348W1 temperature control unit, in rectangular fused quartz cells of 0.2 cm path length at room-temperature with scan range of 190-260 nm and 601 data point for each scan. Result are presented as an average of four scans with scanning speed of 50 nm/min at 0.5 nm increments with an averaging time of 2 s and 1 nm bandwidth with 2 point average. It was not possible to record the CD spectra in chloroform, the solvent used for NMR studies, due to its strong absorption in the region of interest (190-260 nm). Thus the studies were carried out in peptide concentration of ~ 0.2 mM solution in MeOH. All spectra are background subtracted and binomial method was used for smoothening with smoothing window of 99 points. The values are expressed in terms of $[\theta]$, the total molar ellipticity ($deg \cdot cm^2 \cdot dmol^{-1}$).

The CD spectra of **3-5** (Figure 38) in MeOH showed distinct negative maxima at about 198 nm. Though for **3** the absorption is weak, **4** and **5** display the negative maxima with significantly large molecular ellipticities [θ]. These oligomers also contain broad shoulders at higher wave lengths. These features support left-handed 11/9-helices for these peptides in methanol.

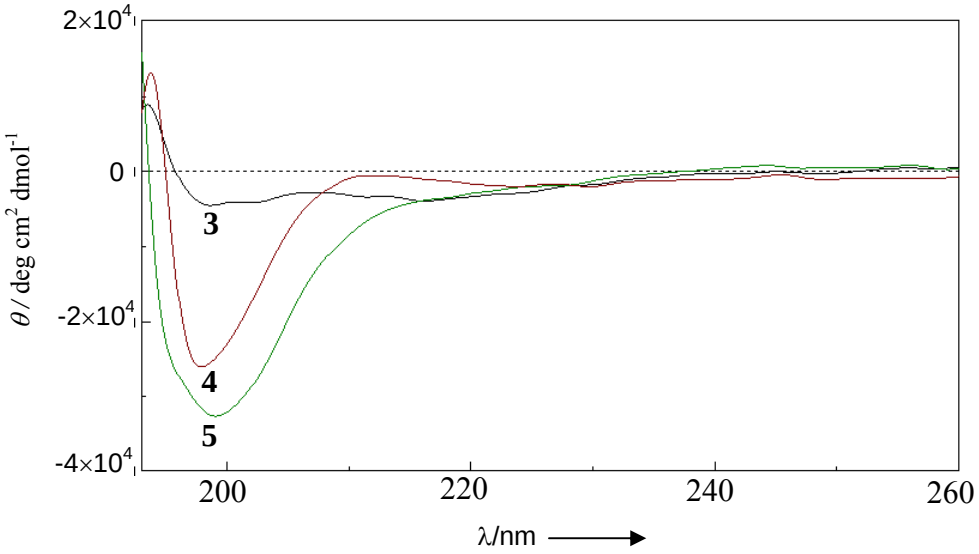

Supporting Figure 38: CD spectra of peptides **3-5** in MeOH.